

2009

Development of methodology for the use of multi-bed sorbent traps with gas chromatography time of flight mass spectrometry

Siva Maheswara Reddy Anna Pareddy

Follow this and additional works at: <http://commons.emich.edu/theses>

 Part of the [Chemistry Commons](#)

Recommended Citation

Reddy Anna Pareddy, Siva Maheswara, "Development of methodology for the use of multi-bed sorbent traps with gas chromatography time of flight mass spectrometry" (2009). *Master's Theses and Doctoral Dissertations*. 144.
<http://commons.emich.edu/theses/144>

This Open Access Thesis is brought to you for free and open access by the Master's Theses, and Doctoral Dissertations, and Graduate Capstone Projects at DigitalCommons@EMU. It has been accepted for inclusion in Master's Theses and Doctoral Dissertations by an authorized administrator of DigitalCommons@EMU. For more information, please contact lib-ir@emich.edu.

Development of methodology for the Use of Multi-bed Sorbent Traps with Gas
Chromatography Time of Flight Mass Spectrometry

By

Siva Maheswara Reddy Anna Pareddy

Dissertation

Submitted to the College of Arts & Sciences

Eastern Michigan University

in partial fulfillment of the requirements for the degree of

Doctor of Philosophy

In

Chemistry

April 14, 2009

DEDICATION

To

My Family, Kiran, Rajesh, Mahender, Venkat, and Kamala (Bujamma).

ACKNOWLEDGEMENTS

I would like to express my deep and sincere gratitude to my supervisor, Dr. Heather Holmes. Her wide knowledge and her logical way of thinking have been of great value for me. Her support, guidance, patience, understanding, and encouragement have provided a good basis for the present thesis.

I am deeply grateful to my committee members, Dr. Ruth Ann Armitage and Dr. Harriet Lindsay.

I owe my most sincere gratitude to Dr. Krishnaswamy Rengan, who directed me towards this research work. I also would like to thank him for his support during my study in the Chemistry department.

I would like to thank the Head of the Chemistry Department, Dr. Maria Milletti, for her support and time in helping with this thesis. I also express my gratitude to the Department of Chemistry at Eastern Michigan University and the Graduate School for my research assistanceship.

The chain of my gratitude would be definitely incomplete if I forgot to thank all of my friends and research group members at the Eastern Michigan University. My deepest and sincere gratitude for all of them for their help during this research work.

ABSTRACT

The lipid peroxidation of unsaturated fatty acids in cellular membranes leads to the formation of alkanes, aldehydes, alkanals, alk-2-enals, and hydroxyl alkenals. The free radicals formed during the process of lipid peroxidation can react with and damage cellular components. Lipid peroxidation is known to cause a number of diseases such as cancer, diabetes, and heart disease. Various analytical methods that include spectrometric assays and chromatographic analyses of derivatized products are available for the detection of the lipid peroxidation products.

The development of rapid, non-invasive monitoring of reactions occurring in biological systems, such as cell cultures, is highly desirable, as such analyses could yield reaction profiles in near-real time. In this study, the utility of a multibed sorbent trap was explored for potential use as a preconcentration step in the analysis of volatile products of lipid peroxidation in biological systems. The trap was integrated into a fully-automated system in which samples are drawn to the trap via vacuum and injected into the GCMS. Results of these studies indicate that a sorbent trap- based inlet system coupled with GCMS should prove useful in the near-real time detection of volatile organic compounds from biological samples.

TABLE OF CONTENTS

DEDICATION.....	i
ACKNOWLEDGEMENTS.....	ii
ABSTRACT.....	iii
LIST OF TABLES.....	vi
LIST OF FIGURES.....	vii
CHAPTER 1: INTRODUCTION	1
1.1 Lipids and their biological function.....	1
1.2 Lipid Peroxidation and diseases.....	4
1.3 Methods to assess lipid peroxidation.....	7
1.4 Gas Chromatography.....	10
1.5 Gas Chromatography Time-of-Flight Mass Spectrometry.....	14
1.6 Research Goal.....	16
CHAPTER 2: EXPERIMENTAL	
2.1 Instrumentation.....	17
2.1.1 Sorbent Trap Development.....	17
2.1.2 Sorbent Trap Assembly.....	18
2.1.3 Sorbent Trap Characteristics.....	20
2.1.4 Typical Automation Parameters.....	23
2.2 Materials and Procedures.....	24
2.2.1 Compounds of Interest.....	25
2.2.2 Standard Solutions.....	26

CHAPTER 3: RESULTS AND DISCUSSION

3.1 Measurement of Blanks.....27
3.2 Bag Sampling.....30
 3.2.1 Data for 1Liter bag sampling.....31
 3.2.2 Data for 5 Liter bag sampling.....35
 3.2.3 Data for 100 Liter bag sampling.....38

CHAPTER 4: CONCLUSIONS.....42

CHAPTER 5: DESIGN OF A METAL CLOSING

5.1 Design of metal closing for the Use of Multibed Sorbent Traps GC-TOFMS.....43

REFERENCES.....46

LIST OF TABLES

Table 2.1. Adsorbents used in the multibed sorbent trap and their properties.....	20
Table 2.2. Volatile compounds used in test mixtures	25
Table 2.3. Dilution scheme for standards of hexanal in the range of 5 to 1 ppm v/v prepared from 10 ppm hexanal solution.....	26

LIST OF FIGURES

Figure 1.1. General structure of fats and oils. The R can be long-chain saturated or unsaturated hydrocarbon groups	1
Figure 1.2. Classification of common phospholipids, glycolipids, and triacylglycerides...	2
Figure 1.3. Structure of a phosphatidylcholine	3
Figure 1.4. Structure of membrane lipid	3
Figure 1.5. Mechanism of the formation of lipid peroxidation products	6
Figure 1.6. Outline of the different methods for the measurement of lipid peroxidation products	8
Figure 1.7. Schematic of a gas chromatograph.....	11
Figure 1.8 Schematic of a Time of Flight Mass spectrometer.....	15
Figure 2.1. Schematic representation of sorbent trap assembly	19
Figure 2.2. Sorbent trap components.....	21
Figure 2.3. Sorbent bed characteristics	22
Figure 2.4. Summary of the Automation Program and Typical Parameters.....	24
Figure 3.1. Chromatogram for room blank.....	28
Figure 3.2. Chromatogram for bag blank.....	29
Figure 3.3. Chromatogram for trap blank.....	29
Figure 3.4. Bag sampling of the mixture	30
Figure 3.5. Chromatogram for the mixture at 15 sec for 1L bag sampling	32
Figure 3.6. Chromatogram for the mixture at 20 sec for 1L sampling	32

LIST OF FIGURES (CONTINUED)

Figure 3.7. Chromatogram for the mixture at 25 sec for 1L bag sampling33

Figure 3.8. Chromatogram for the mixture at 30 sec for 1L bag sampling33

Figure 3.9. Chromatogram for the mixture at 40 sec for 1L bag sampling34

Figure 3.10. Chromatogram for the mixture at 60 sec for 1L bag sampling34

Figure 3.11. Chromatogram for the mixture at 15 sec for 5L bag sampling35

Figure 3.12. Chromatogram for the mixture at 20 sec for 5L bag sampling36

Figure 3.13. chromatogram for the mixture at 30 sec for 5L bag sampling36

Figure 3.14. Chromatogram for the mixture at 40 sec for 5L bag sampling37

Figure3.15. Chromatogram for the mixture at 50 sec for 5L bag sampling37

Figure 3.16. Chromatogram for the mixture at 60 sec for 5L bag sampling38

Figure 3.17. Chromatogram for the mixture at 20 sec for 100L bag sampling39

Figure 3.18. Chromatogram for the mixture at 30 sec for 100L bag sampling39

Figure 3.19. Chromatogram for the mixture at 40 sec for 100L bag sampling40

Figure 3.20. Chromatogram for the mixture at 60 sec for 100L bag sampling40

Figure 5.1. Metal closure system with four port valve and sorbent trap.....43

Figure 5.2. Cross sectional view of the metal closure.....44

CHAPTER 1

INTRODUCTION

1.1 Lipids and their biological function

A lipid is defined as a water insoluble biomolecule that has a high solubility in nonpolar organic solvents such as chloroform. The simplest lipids are the fats, which are triesters made up of one glycerol backbone with three fatty acids. The general structure of fats and oils is shown in Figure 1.1. The lipids can be classified into four different groups:

1. Simple lipids such as fats, oils, and waxes
2. Compound lipids such as phospholipids, sphingolipids, and glycolipids
3. Sterols such as cholesterol and several hormones
4. Fat-soluble vitamins A, D, E, and K

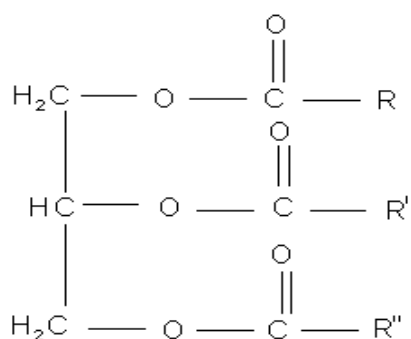


Figure 1.1. General structure of fats and oils. The R can be long-chain saturated or unsaturated hydrocarbon groups.

Triacylglycerols are used largely for energy storage in animals. More complex lipids, the phospholipids, glycolipids, and cholesterol, are the major constituents of biological cell membranes. The classifications of common lipids are shown in Figure 1.2.

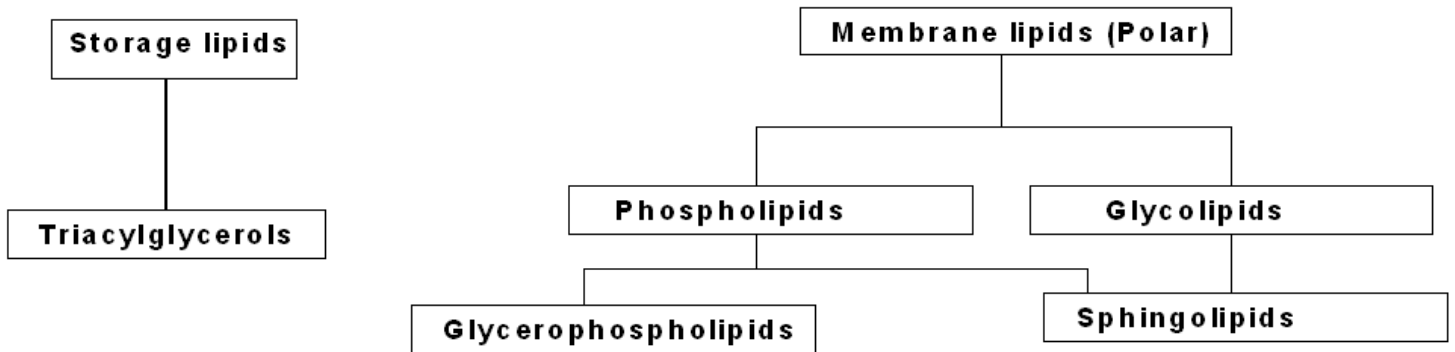


Figure 1.2. Classification of common phospholipids, glycolipids, and triacylglycerides.

In mammals, the cytoplasm of adipose cells is the major reservoir of triacylglycerols [1]. A mammalian fat cell consists of a small droplet of condensed triacylglycerols enclosed by a thin cell membrane with the cell nucleus bulging out to one side [2]. Most of the energy reserve of animals is stored in fat cells. The lipid bilayer of cellular membranes mainly consists of phosphatidylcholines. The lipid bilayer structures are shown in Figure 1.3. The polar head group of the layer is water soluble and contains the negatively charged phosphate group and positively charged nitrogen in choline and shapes the inner and outer surfaces of the membrane [3]. The hydrophobic tail of each molecule points toward the middle of the bilayer [4].

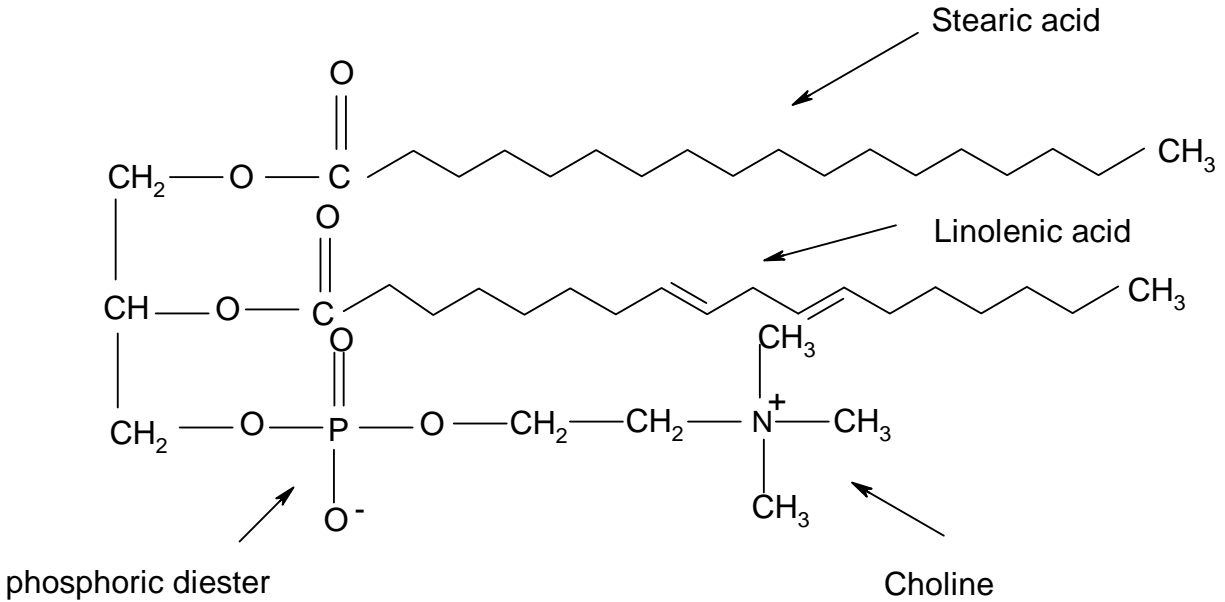


Figure 1.3. Structure of a phosphatidylcholine [4].

Arachidonic acid in phosphatidyl choline is an important component of the cell [5]. The structure of a membrane lipid with arachidonic as an unsaturated group is shown in Figure 1.4; the arachidonic acid is a polysaturated fatty acid with four *cis* double bonds that react with the molecular oxygen.

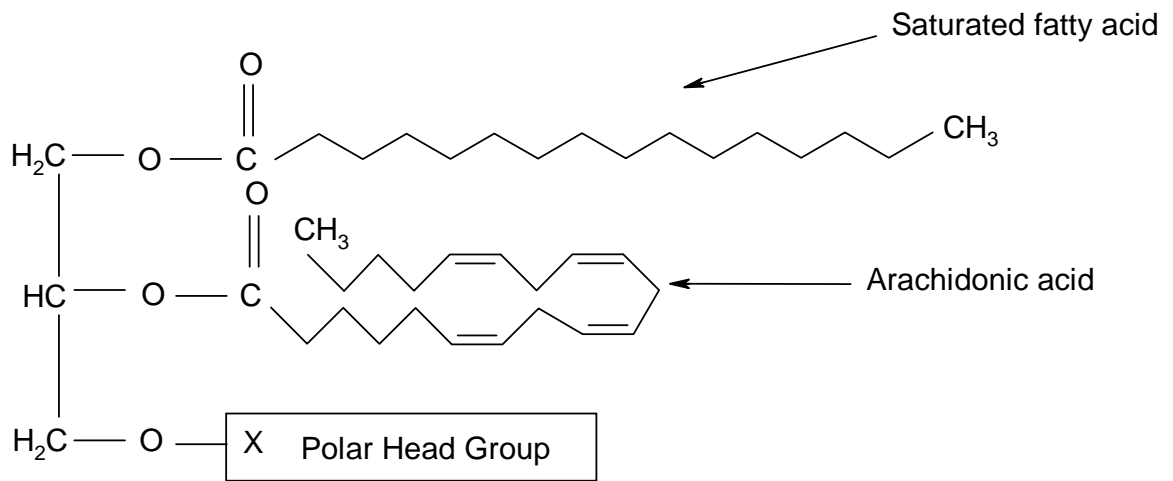


Figure 1.4. Structure of membrane lipid

1.2 Lipid Peroxidation and Diseases

In tissues and tissue fractions, lipid peroxidation is a major degradative process that occurs due to overproduction and propagation of free radical reactions primarily involving membrane polyunsaturated fatty acids [6]. Lipid peroxidation is thought to play a major role in the pathogenesis of various diseases including atherosclerosis, diabetes, cancer, and rheumatoid arthritis as well as in drug induced toxicity, postischemic reoxygenation injury, and aging [6].

One mechanism of the formation of lipid peroxidation products is shown in Figure 1.5. Lipid peroxidation of unsaturated fatty acids in biological cell membranes results in the formation of alkoxy radicals that degrade into different by products such as hexanal, heptanal, pentanal, pentane, malondialdehyde, 4-hydroxynonenal (4-HNE), and the low molecular weight aldehydes [7]. These products are more stable than free radicals

that naturally initiate the process, so they can diffuse inside the cells and cause cell damage.

The number of double bonds and the position of double bonds in the fatty acids play an important role in oxidation and the formation of oxidation products; the more the double bonds, then the greater the oxidation. The closer the first double bond to the methyl terminus, the more the oxidative products will be formed [8, 9]. The peroxidative breakdown of polyunsaturated fatty acids (PUFAs) has also contributed to the pathogenesis of many types of hepatic diseases induced by several toxic substances. Haloalkanes, carbon tetrachloride, trichlorobromomethane, chloroform, dibromoethane, halothane, and in some instances ethanol have been shown to trigger lipid peroxidation [10].

There is growing evidence that aldehydes generated endogenously during the process of lipid peroxidation are usually involved in most of the pathophysiological effects associated with oxidative stress in cell and tissues [11]. Lipid peroxidation derived aldehydes are relatively stable when compared with free radicals and can escape easily from the cell and attack targets far from the site of the original free radical initiated event. For that reason they are not only end products and remnants of the lipid peroxidation process, but also act as mediators for the primary free radicals that initiated lipid peroxidation. Among the lipid peroxidation derived aldehydes, 4-HNE can be produced in large concentrations from arachidonic acid, linoleic acid, or from their hydroperoxides and is primarily responsible for the cytopathological effects observed during the *in vivo* oxidative stress studies [11].

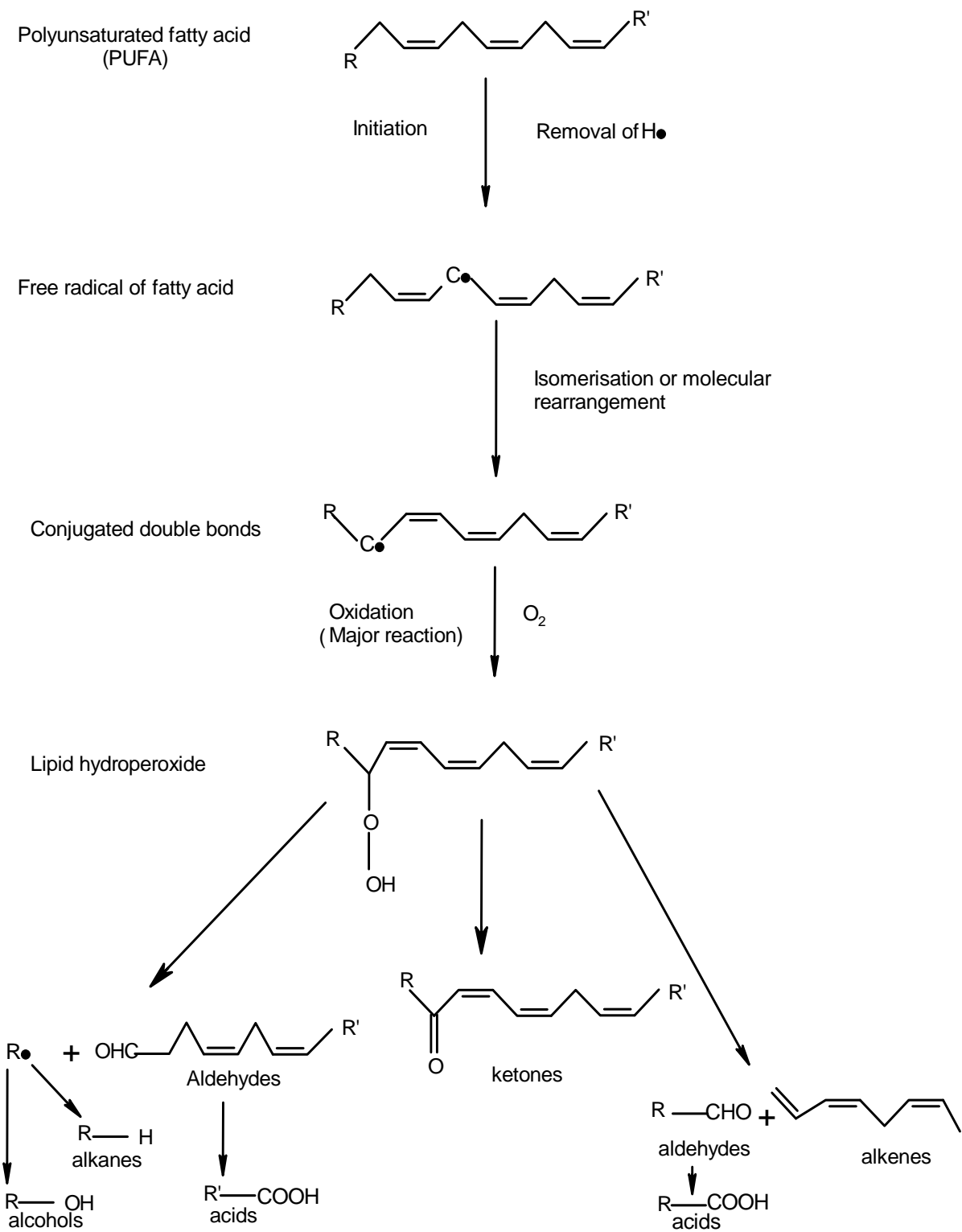


Figure 1.5. Mechanism of the formation of lipid peroxidation products [8].

1.3 Methods to Assess Lipid Peroxidation

Various methods of analysis for lipid peroxidation products have been developed and are shown in Figure 1.6. Each method has its own advantages and disadvantages under given circumstances. Sometimes a combination of these methods is desirable for better sensitivity [12].

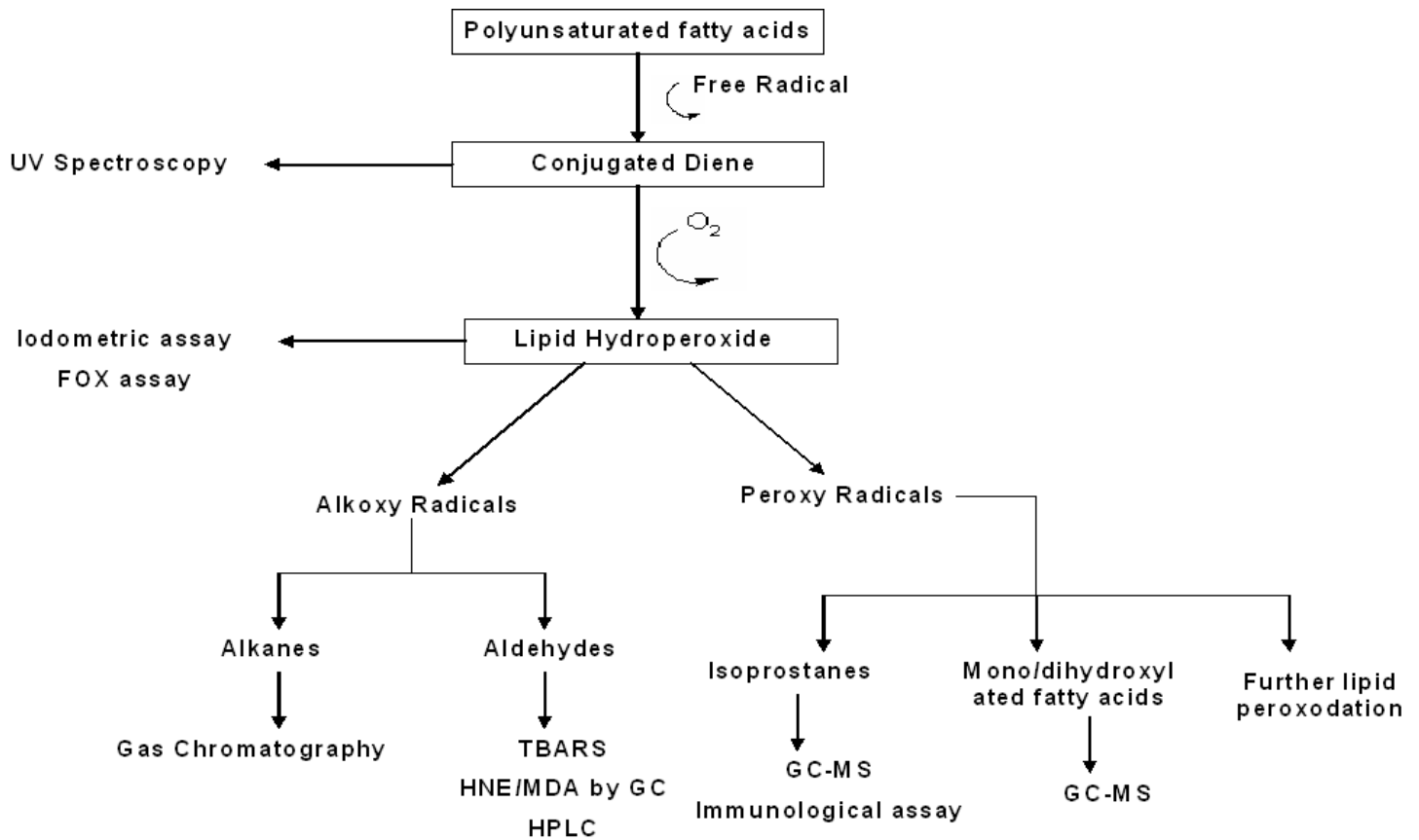


Figure 1.6. Outline of the different methods for the measurement of lipid peroxidation products [13].

It was in 1944 that the thiobarbituric acid – reactive substances (TBARS) test was first introduced by Kohn and Liversedge, and even to date it is one of the most popular tests used for the detection of volatile aldehydes due to its simplicity [14, 15]. In the TBARS assay, the samples are heated in an acid buffer with thiobarbituric acid at a very low pH. During this reaction process, a pink chromogen, which is a thiobarbituric acid-malendialdehyde (TBA-MDA) adduct, is formed. The absorbance of this adduct can be measured by UV spectrometry at 532 nm or by fluorescence at 553 nm [16, 17]. This test is relatively simple and inexpensive. However, in the recent literature the TBARS test has been a topic of criticism from many authors because it is destructive to the sample. Moreover, in the TBARS assay, the overall analysis is run in a non-specific fashion, and only a general measure of the overall extent of lipid peroxidation is possible rather than the identification or quantification of particular aldehyde species. It has also been shown that some aldehydes, especially MDA, can be produced by the reaction conditions rather than by the actual process of lipid peroxidation in the sample [18].

Gas chromatography-mass spectrometry provides a number of other methods for the determination of aldehydes and other lipid peroxidation products in biological samples. One such method described by Luo *et al.* includes the use of *o*-(2,3,4,5,6-pentafluorobenzyl) hydroxylamine hydrochloride (PFBHA.HCL) to form the *o*-pentafluorobenzyl-oxime (PFB-oxime) derivatives of both saturated and unsaturated aldehydes (C₂-C₁₂) including hexanal, 4-HNE, and MDA, followed by trimethylsilylation of the hydroxyl group to trimethylsilyl (TMS) esters. The PFB-oxime-TMS derivatives are then analyzed by capillary column gas chromatography-negative-ion chemical ionization mass spectrometry (GC-NICIMS) with ammonia as reagent gas [19]. The

quantitation of the aldehydes can be done using benzaldehyde-ring-D₅ as an internal standard in selected ion monitoring (SIM) mode. With this it is possible to achieve a detection limit between 50 and 100 fmol/ μ l injected aldehyde. The high sensitivity of this method allows the measurement of physiological aldehyde levels in biological samples and also the products of aldehyde metabolism as well. But with this method, the accurate and simultaneous measurement of HNE and some unsaturated aldehydes in biologicals samples (plasma and tissue homogenates) is difficult because of losses during sample preparation. To solve the accuracy problem, the use of specific, stable isotopic internal standards is recommended [20].

Simultaneous analysis of various aldehydes that are produced due to lipid peroxidation is possible by reducing the aldehydes to stable alcohols [21]. The reduction process is carried out under neutral conditions at room temperature or at 4° C with either sodium borodeuteride (NaBD₄) or sodium borohydride (NaBH₄). After the extraction process the alcohols are converted to *t*-butyldimethylsilyl ethers and are analyzed by selected ion monitoring gas chromatography-mass spectrometry in the positive chemical ionization mode (GC-PICIMS) for malendialdehyde and 4-HNE and electron impact mode for all other aldehydes. Quantitation is achieved using internal standards of 1,3-[²H₈] propanediol for MDA, of 4-[2-²H]hydroxynonenal for 4-HNE, and of the corresponding saturated per-deuterated alcohols for all saturated aldehydes, for example [²H₃] hexanol for hexanal. The main advantage of using saturated per-deuterated alcohols is they serve as external standards for their unsaturated aldehydes with the same chain length. With this method it is possible to achieve the detection limits as low as 0.5 nmol in a given sample. The method is not only highly sensitive and selective but also can be

used to verify the identity of each aldehyde by observing a mass shift when aldehydes are reduced with either NaB_2H_4 or NaBH_4 . The only drawback of this method is control of assay conditions; it is very difficult to control the assay conditions for aldehydes and biological samples, including plasma.

1.4 Gas chromatography (GC)

For more than two decades, GC has been a very useful tool for the separation, detection, and identification of both semi-volatile and volatile organic compounds [22]. The main advantage of GC is its simplicity and ruggedness for rapid, yet complete analysis of mixtures of compounds over a wide range of concentrations with excellent accuracy and Precision [22]. A typical commercially available GC is shown in Figure 1.7, which consists of carrier gas (CG), flow regulator (FR), a sample injector (SI), a column (C), an oven (O) in which the column is placed, an injection port (IP), a detector (D), and a processor (P). In a gas chromatographic analysis, minute amounts of sample are injected into a stream of continuously moving carrier gas, which is the mobile phase. Nitrogen, helium, and hydrogen are generally used. The sample is carried by the stream through a column that consists of a tube containing a stationary phase, which can be a solid or a liquid [23]. Separation of a sample mixture into its individual components is achieved due to differences in the affinity of the stationary phase for each component and by optimizing column temperature and the carrier gas flow rate. A bypass valve allows carrier gas to flow to the detector in order to minimize dead volume [22].

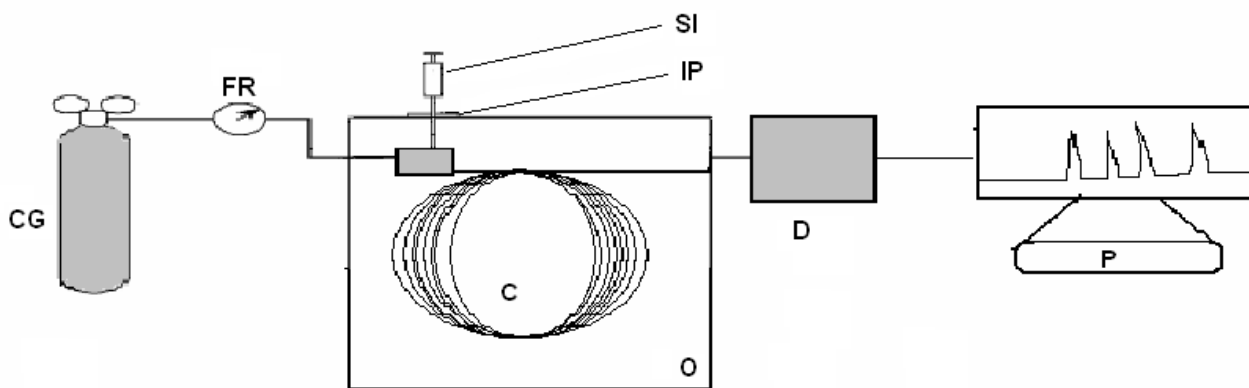


Figure 1.7. Schematic of a gas chromatograph.

The columns used in the separation of compounds by GC are of two types, packed and capillary columns. Column materials, internal diameter, and film thickness are important factors. Packed GC columns are fabricated from glass, metal, or Teflon tubes that have lengths of 2 to 3 m and inside diameters of 2 to 4 mm. Packed columns separate simple mixtures rapidly, but the resolving power for complex mixtures is limited. Resolution of peaks can be improved with an increase in the column length, but the analysis time increases proportionally.

Capillary columns made of fused silica are widely used for the separation and analysis of low molecular weight compounds [24]. There are two basic types of capillary columns available, wall coated open tubular (WCOT) and support coated open tubular (SCOT). The WCOT are capillary tubes that are coated with a thin layer of stationary phase. In SCOT, the inner surface of the capillary is lined with a thin film of a support material coated with stationary phase, greatly increasing the surface area and hence the volume of the stationary phase. With SCOT larger samples can be analyzed in trace analysis without saturating the stationary phase. The disadvantages of SCOT include that it is less efficient than WCOT. With WCOT, large volume of samples can be

analyzed but the limitations of using WCOT GC is the prolonged analysis time for certain applications. Typical analysis time is 20 to 30 minutes, which restricts the use of WCOT GC in important areas such as environmental monitoring in which rapid sample analysis is desired. A decrease in analysis time can be achieved by using a short column, high carrier gas flow rate, and a fast detector and injection technique. Sacks et al. used a combination of a tandem column ensemble and an on-line microdesorption trap for the analysis of organic compounds in biological samples; with this method low detection limits can be obtained for several volatile compounds in biological samples [25, 26]. Gas-cooled and electrically heated cryofocusing inlet systems with a miniature incubator have been extensively used with fast GC to analyze compounds under high-speed conditions [27].

Static and dynamic headspace techniques have also been used for the analysis of volatile organic compounds [28-30]. In static headspace sampling, the sample containing volatile organic compounds is allowed to equilibrate with its headspace gas in a sealed container at a constant temperature. This technique is limited because of high detection limits and also requires thermodynamic equilibrium of the sample with its headspace [31]. In dynamic headspace analysis, also known as purge and trap, the sample is drawn to a sorbent bed prior to injection to the GC. The sample is desorbed by heating the trap and then transferring the vapor plug to the GC system. This technique offers better sensitivity and solvent free operation [32]. With this technique, most of the volatile organic compounds can be quantitatively determined, but the method is limited because of lengthy sample preparation and analysis times [16].

Frankel et al. used static headspace GC for the determination of volatile organic compounds such as hexanal as an indicator of n-6 PUFA peroxidation in rat liver samples and red blood cell membranes of humans. This method can separate and identify complex mixtures in one tenth of time of conventional GC. Also, differentiation of n-6 PUFA (hexanal and pentane) and n-3 PUFA (propanal) peroxidation products is possible [15].

The dynamic headspace capillary GC method is a very rapid and sensitive technique for the simultaneous analysis of low molecular weight volatile organic compounds, especially hexanal and pentanal [34]. With this method it is possible to make up to 15 determinations per one hour. This method has been extensively used to determine hexanal as a lipid peroxidation product in oil and oil-based foods that have spoiled due to improper storage.

Jiankang et al. compared the GC-MS/NCI (Negative Chemical Ionization) method and TBARS test for the analysis of malondialdehyde with 13 unsaturated fatty acids and biological samples such as heart, liver, kidney, plasma, and neural cells. The results of the study indicated that these two methods gave almost parallel results, but the GC-MS/NCI ensured better sensitivity and selectivity than the TBARS assay. The GC-MS/NCI also offered additional advantage of efficient processing of large number of samples and the elimination of recovery errors because of the inclusion of internal standard [35].

1.5 Gas Chromatography (GC)Time-of-Flight (TOF) Mass Spectrometry (MS)

Mass spectrometry is an analytical technique that measures the mass-to-charge ratio (m/z) of ions generated by the fragmentation of molecules. The generated mass spectrum is a plot of the ion abundance as a function of m/z . It is a very specific and widely used technique to achieve low detection limits of the compounds [36].

Typical analysis times for standard GC-MS measurements can easily range from 30 minutes to well over 1 hour. In an effort to reduce the analysis time and at the same time maintain the superior qualitative information of a mass spectrometric measurement, analytical chemists have looked at the applicability of faster GC separations in combination with swift MS detection.

In a TOFMS, the m/z ratio of an ion is determined by measuring an ion's travel time from the ion source to the detector. A typical schematic of a TOFMS is shown in Figure 1.8. Ions arrive at the detector at different times depending on their masses. Ions created in the source travel through the push pulse electrode. Electric potential differences between the push pulse electrode and the accelerator electrode create an electrical force that accelerates the ions to the same kinetic energy. Since the ions have very close to the kinetic energy, their velocities depend only on m/z ratio; thus the heavier the ion, the longer its time-of-flight.

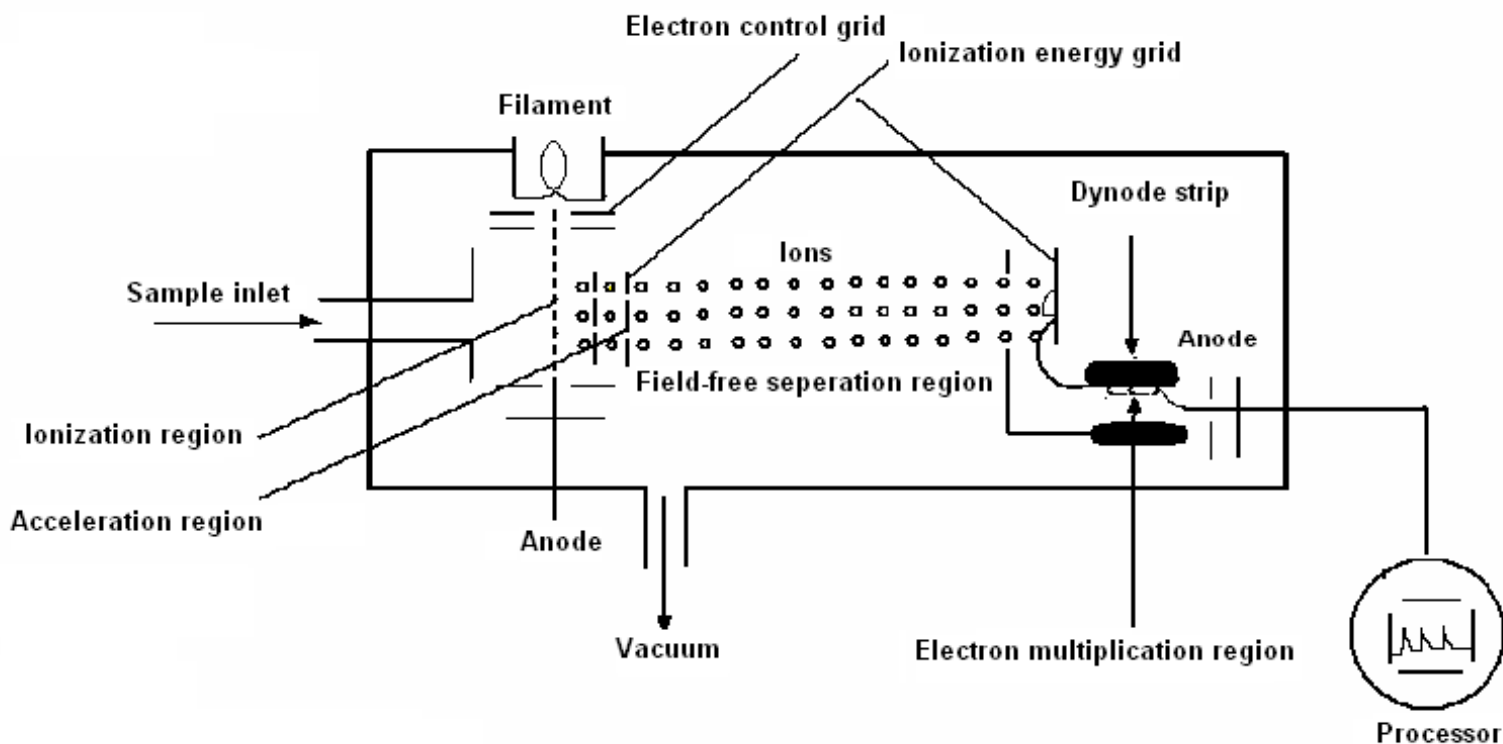


Figure 1.8. Schematic of a time of flight mass spectrometer.

Time-of-flight mass spectrometers have a number of advantages such as the dramatic reduction of analysis time and improved quality of the analytical results [37]. A TOFMS with a high-speed recorder and an optimized ion extraction technique offers the fastest way to acquire a mass spectrum [38, 39]. In TOFMS, the highest mass under analysis limits the time to acquire a mass spectrum because of the longest flight time. For GC-TOFMS purposes, a full spectrum can be collected in under 100 μs . However, a single spectrum will not possess the required signal-to-noise ratio (S/N). In order to improve the S/N, a number of spectra must be averaged. A time array detection scheme with an integrating transient recorder has been developed for spectral acquisition on a rapid scale [40-42].

1.6 Research Goal

The goal of this research was the development of a rapid and non-invasive sampling method for biological samples (i.e., cell cultures) in order to observe the reactions and measure the resulting products in near-real time. In this study, the utility of a multibed sorbent trap was explored for potential use as a preconcentration step in the analysis of volatile products of lipid peroxidation in biological systems. The sorbent trap was integrated into a fully-automated system in which samples are drawn to the trap via vacuum and injected to the GCMS.

CHAPTER 2

EXPERIMENTAL

2.1 Instrumentation

2.1.1 Sorbent trap development

Sorbent traps have been developed as automatic sampling and injection devices for continuous, on-line GC analysis of VOCs for biological and other applications [43-46]. Sorbent traps are small capillary tubes with an internal diameter of around 0.5 mm packed with adsorbents such as graphitized carbon. As VOCs are drawn through the trap they are adsorbed by the packing material. The adsorbed VOCs can be rapidly desorbed by resistive heating using a pulse of electric current to make an injection for a GC separation. The major advantage of using a sorbent trap as an injection device for the analysis of VOCs is that it acts as a sample preconcentrator, which allows larger volumes of gaseous samples to be analyzed for trace measurements.

The sorbent trap can retain low heat capacity and can be heated or cooled very rapidly. The trap is heated resistively, so heat can transfer from the external tube wall into the sorbent bed. Fast desorption is very important to achieve high resolution separation by the generation of narrow injection bands. The transfer in larger diameter traps takes a longer time and desorption of VOCs is slower, causing wider injection bandwidths. However, due to its microdimensions, a trap can only be packed with a small quantity of sorbent. The ideal sorbent would be the one that has large sampling capacity or breakthrough volume for the very VOCs and at the same time provides rapid, quantitative desorption of the large molecular compounds. It is necessary to accumulate as much

sample as possible in the sorbent trap prior to making an injection in order to make trace analysis possible. If a component in the trap breaks through (i.e., the retaining power of the sorbent is insufficient or overwhelmed by sample such that sample is lost during the trapping process), only a fraction of the sample is desorbed during injection, generating a smaller signal at the detector. As the sorbent trap contains only a small quantity of sorbents, it can be prone to breakthrough problems. The breakthrough volume for the sorbent trap is a function of the amount of the adsorbent and its strength. Increasing the mass of sorbent in the trap can result in the larger breakthrough time of the trap at a given flow rate. A larger diameter trap can hold more adsorbent but requires longer desorption times than smaller diameter traps due to the slower heat transfer in larger traps compared to smaller traps.

2.1.2 Sorbent trap assembly

Figure 2.1 shows the experimental setup developed for this research. The setup consists of a sampling system, the sorbent trap coupled with a GC-MS. The flow of the analytes to the system is controlled by a 4-port valve (V1). Valve (V2) opens in order to draw the sample (S) on to the sorbent trap. Valve (V3) is used to control the carrier gas (CG) that is necessary to send the absorbed components on to the GC column. During the sampling mode (Fig. 2.1a), sample (from S) is drawn to the trap through V1 via vacuum while V2 is open and V3 is closed. After the sampling period (Fig. 2.1b), valve V3 is opened and valve V2 is closed, allowing carrier gas to sweep through the trap to the GC-MS by V1 while the connection to the sorbent trap is closed. The sample is connected to ambient pressure air and the connection to the sorbent trap is closed by switching V1.

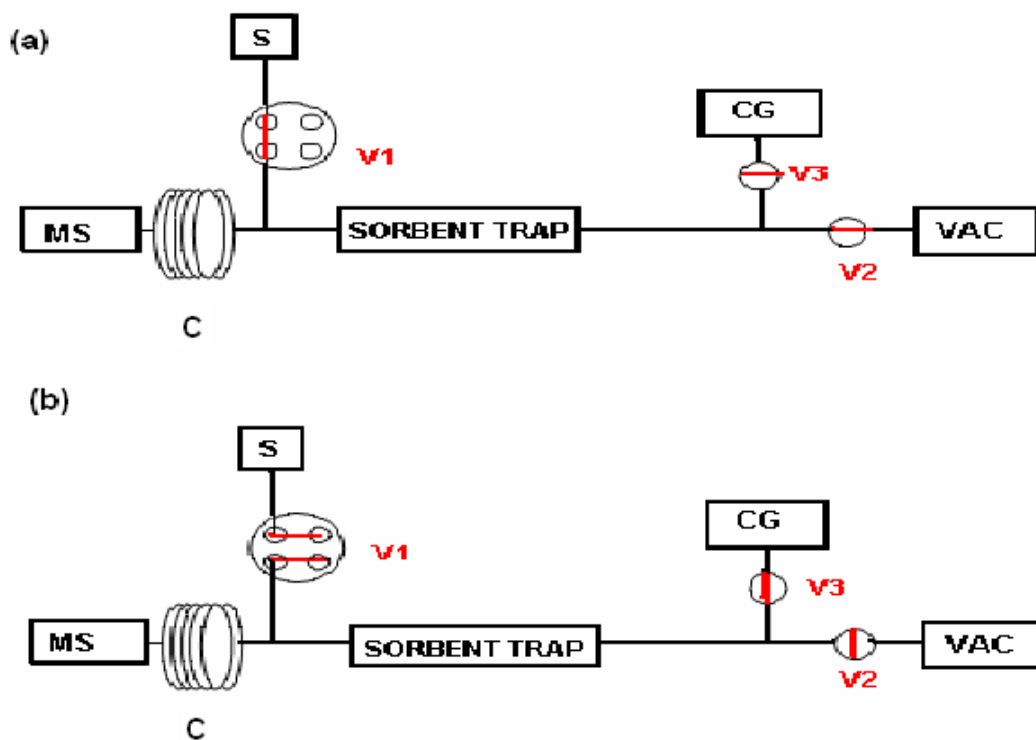


Figure 2.1. Schematic representation of sorbent trap assembly. (a) Sampling mode: Sample S is drawn to the sorbent trap via vacuum*. (b) Analysis mode: Carrier gas CG moves sample from sorbent trap through column C to the mass spectrometer when the trap is rapidly heated**.

* Through valves V1 and V2, valve V3 is closed.

** Valve V3 is open, while valve V2 is closed

After an equilibration period, the trap is heated rapidly using AC current, and the analytes are injected onto the separation column and MS. The main reason for equilibrating the system is that during the sampling mode there is influx of air that enters into the system, and the oxygen in the air is thought to be the main source of background noise as well as causing rapid filament burnout in the MS. The equilibration period is intended to clear oxygen from the MS before the analysis mode.

2.1.3 Sorbent trap characteristics

The sorbent trap developed for this research was modeled after Sacks et al [48]. The design and inner compartments of the trap are shown in Figure 2.2. The trap is 80-mm-long, 1.35-mm-I.D. tube made of Inconel 600, a Nickel-Copper (Ni-Cu) alloy (Accu-Tube Corp., Englewood.CO). Adsorption beds labeled B, X, and Y correspond to the three commercially available adsorption materials (Supelco., Bellefonte, PA) described in Table 2.1.

Table 2.1. Adsorbents used in the multibed sorbent trap and their properties.

Symbol	Adsorbent	Mesh size	Surface area (m ² g ⁻¹)	Density (g mL ⁻¹)	Application
B	Carbopack B	60/80	100	0.36	C ₅ -C ₁₂
X	Carbopack X	40/60	250	0.41	C ₃ -C ₅
Y	Carbopack Y	40/60	25	0.42	C ₁₂ -C ₂₀

About 2.2 mg of each material was used to form the beds. This quantity has been shown to prevent breakthrough of a number of volatile and semi-volatile compounds at the concentrations used in this work. [47,48].

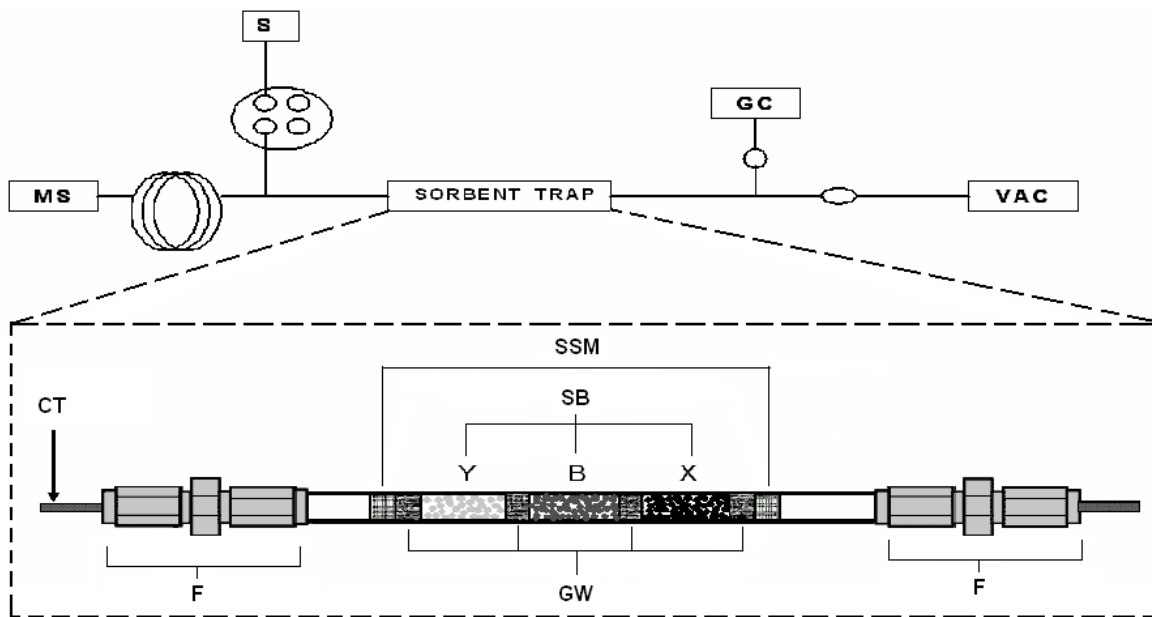


Figure 2.2. Sorbent trap components. SB: sorbent beds; GW: glass wool; SSM: stainless steel mesh; F: stainless steel fitting; CT: connecting tubing.

The adsorption strength of the beds as shown in Table 2.1 reveals X as the strongest, B as the intermediate, and Y as the weakest. During the sample collection, or preconcentration, the sample flow is from left to right through the trap tube as shown in Figure 2.3. The highest boiling point components are trapped in the first and weakest adsorbent. Sorbent bed B, a somewhat stronger adsorbent, retains medium-sized molecules, while sorbent bed X (the strongest) retains the more volatile analytes. During the analysis mode, the sample flow is from right to left, and the higher boiling point compounds are quantitatively removed by the first bed(s) and, thus, they never reach the strongest bed (i.e., X), from which they would be very difficult to desorb as a narrow vapor plug. Each bed is separated by glass wool plugs to prevent mixing, and stainless steel mesh is used to lock up the ends of the three bed assembly.

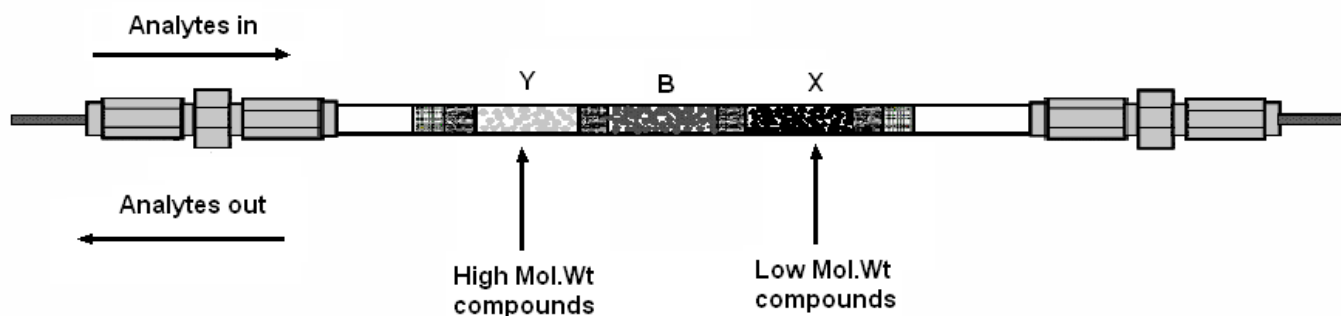


Figure 2.3. Sorbent bed characteristics. High molecular weight compounds are trapped on the weakest bed, Y. Because the flow is reversed prior to desorption, high molecular weight compounds do not contact the stronger beds B and X from which they might not quantitatively desorb.

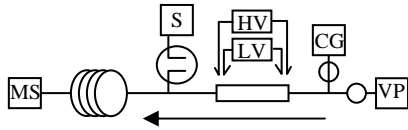
The trap was terminated at both ends with 0.25 mm-I.D fused silica tubing by means of low dead volume metal fittings. During the sample analysis, the flow rate of sample gas through the trap was typically 45-85 cm³/min, as determined by the vacuum pump and pneumatic restriction between the pump and atmospheric pressure sample. A type-J thermocouple using 0.127 mm-I.D. wire (36 AWG, Omega Engineering, Stamford, CT) attached to the outer wall of the tube was used to monitor the trap temperature. To maintain a constant operating temperature for several seconds, the trap tube was resistively heated by a two- step heating process using a moderately high current and a short duration pulse for rapid heating and a longer duration, lower current pulse to maintain the maximum temperature. For the trap automation, a separate program in LABVIEW was used on a different computer. Both systems were connected by using a 16-bit A/D board (CIO-DAS16/F, Measurement Computing Corp., Middleboro, MA). Two adjustable autotransformers were used to supply ac power for trap heating, since the very low resistance of the trap tube made the use of a dc supply more difficult.

Approximately 12V current was applied for 0.25 s for very rapid heating with minimal overshoot, and 2V current was applied to maintain the trap temperature for approximately 5 s to ensure complete desorption of the sample and to minimize the contamination of the trap by traces of high boiling point impurities in the analyte mixture.

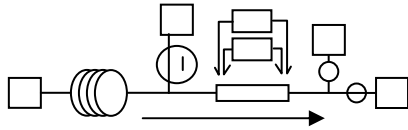
2.1.4 Typical Automation Parameters

Figure 2.4 shows an example of the input screen developed using LABVIEW software for the automation of the sorbent trap inlet system. During mode 1, the system is in “standby” between analysis, configured such that carrier gas flow is in the forward direction through the system as shown in Fig 2.3. When the signal input is given for the analysis to begin, a standby (mode 1) occur prior to sampling (mode 2), from then onwards equilibration (mode 3), high voltage (mode 4), low voltage (mode 5), and analysis/standby (mode 6) are followed.

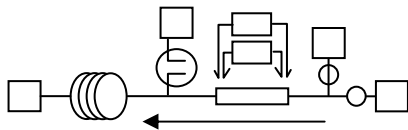
Mode 1: Standby



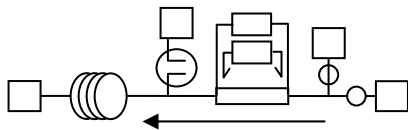
Mode 2: Sampling



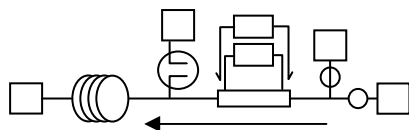
Mode 3: Equilibration



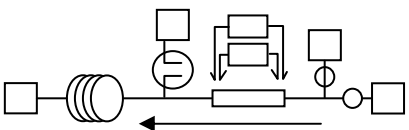
Mode 4: High Voltage



Mode 5: Low Voltage



Mode 6: Analysis/Standby



**Entered
Parameters:**

0.00

Sampling
occurs for
60.00 s

60.00

Equilibration
occurs for
30.00 s

90.00

High Voltage is
applied for 0.25 s

90.25

Low Voltage is
applied for 0.75 s

91.00

Figure 2.4. Summary of the Automation Program and Typical Parameters

2.2 Materials and Procedures

2.2.1 Compounds of interest

Table 2.2 shows the test compounds and their boiling points. Samples were prepared in 1-L, 5-L, and 100-L Tedler gas sampling bags by injecting microliter quantities of a mixture or individual components and diluting with nitrogen. For all the studies, sample collection times in the range of 15-60 s were used with different sample gas flow rates ranging from 40 to 50 cm³/min.

Table 2.2. Volatile compounds used in test mixtures

Compound Name	Structural Formula	Molecular Weight	Boiling Point, °C
Hexane	C ₆ H ₁₄	86.18	69
Heptane	C ₇ H ₁₆	100.2	98.4
Octane	C ₈ H ₁₈	114.23	125-127
Nonane	C ₉ H ₂₀	128.26	150.8
Hexanal	C ₆ H ₁₂ O	100.16	131
Heptanal	C ₇ H ₁₄ O	114.19	153
Pentanal	C ₅ H ₁₀ O	86.14	103

Hydrogen carrier gas was purified with filters for moisture, hydrocarbons, and oxygen. The pressure was varied depending on the gas bag volume, but the typical inlet pressure was between 40-70 psi. Care was taken to maintain the equilibration time in between the sampling and analysis modes to get rid of the oxygen that entered during the sampling.

2.2.2 Standard Solutions

Sodium acetate buffer, pH 6.5 (Mallinckrodt, Paris, KY, U.S.A.) was prepared by diluting the required mass of anhydrous sodium acetate (NaAc, FW 82.03 g/mol) in distilled, deionized (DI) water. The desired pH was attained by adding concentrated HCl, while monitoring with a pH meter. Standard solutions of hexanal were made by mixing 1 μL of hexanal (98%, Sigma Aldrich Co., Saint Louis, MO.) with 10 mL of 0.1 M sodium acetate buffer, pH 6.5. Several vials of this 100 ppm v/v standard solution were stored at $-20\text{ }^{\circ}\text{C}$. This was the only standard that was stored. The 100 ppm solution was wrapped in foil and kept on ice at all times after removal from the freezer. Standard solutions of 10 ppm v/v in sodium acetate buffer with pH 6.5 were prepared fresh whenever needed from the 100 ppm v/v stock. Table 2.3 shows the dilution scheme for hexanal in the range of 1 to 5 ppm v/v.

Table 2.3. Dilution scheme for standards of hexanal in the range of 5 to 1 ppm v/v prepared from 10 ppm hexanal solution.

Hexanal Concentration (ppm)	Amount of 10 ppm (μL)	Amount of buffer (μL)
5	125	125
4	100	150
3	75	175
2	50	200
1	25	225

CHAPTER 3

RESULTS AND DISCUSSION

3.1 Measurement of Blanks

In order to assess the quality and reproducibility of the measurements with bag sampling, three types of blank measurements were run prior to collecting data each day. These included ambient air (room blank), sampling bag containing only nitrogen (bag blank), and assessment of trap degradation (trap blank).

Room blanks were run using a sampling time of 1 minute to allow the air to enter into the trap system. Chromatograms were collected for 5 minutes. A representative for a room blank is shown in Figure 3.1. Chromatograms from room blanks showed a small peak at 95 seconds and a cluster of peaks near 150 seconds. While the room blank did vary somewhat from day to day, the maximum peak height for room blanks was typically less than 60,000 ion counts, as shown in Figure 3.1.

Bag blanks were run by filling a 5 L Tedler bag with nitrogen and sampling it for 1 minute chromatograms were collected for 5 minutes. A representative chromatogram for a bag blank is shown in Figure 3.2. The resulting chromatograms from the bag blanks also showed only peaks at 95 seconds the peaks near 150 seconds and some background noise.

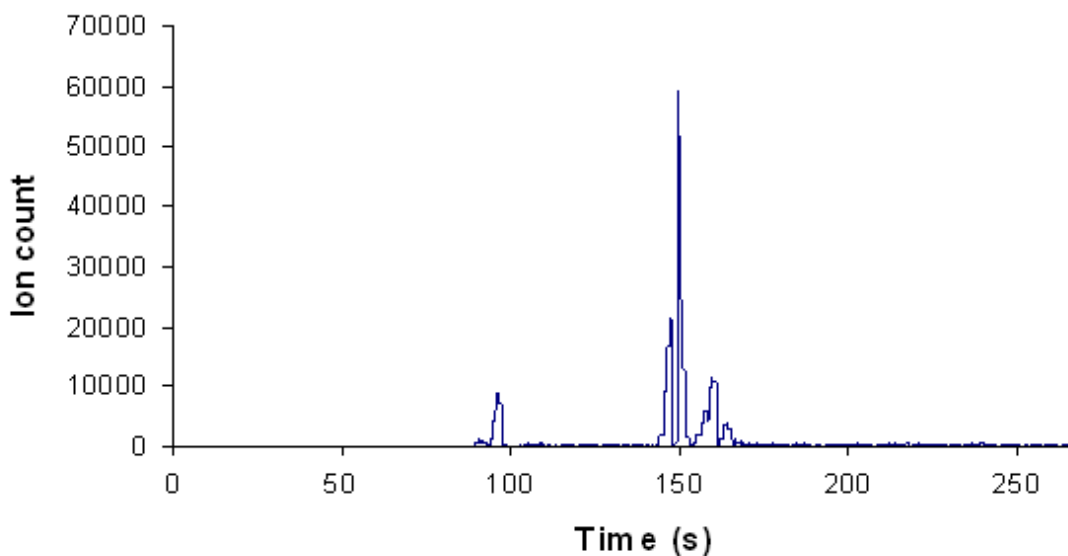


Figure 3.1. Chromatogram for room blank

Trap blanks were run by closing the sampling system and desorbing the trap contents into the GC-MS systems. Chromatograms were collected for 3 minutes. A representative chromatogram for a trap blank is shown in Figure 3.3. The resulting chromatograms from the trap blanks showed only a large peak at 65 seconds and a few smaller peaks. It is notable that in the absence of sampling, the peaks at 95 and 150 seconds were not present.

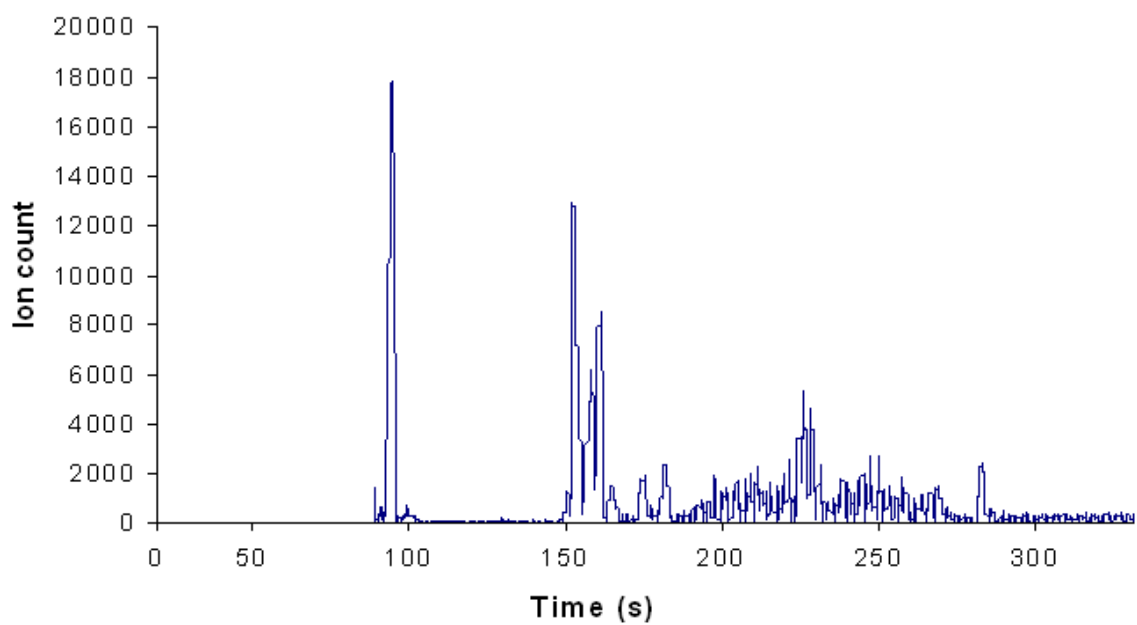


Figure 3.2. Chromatogram for bag blank

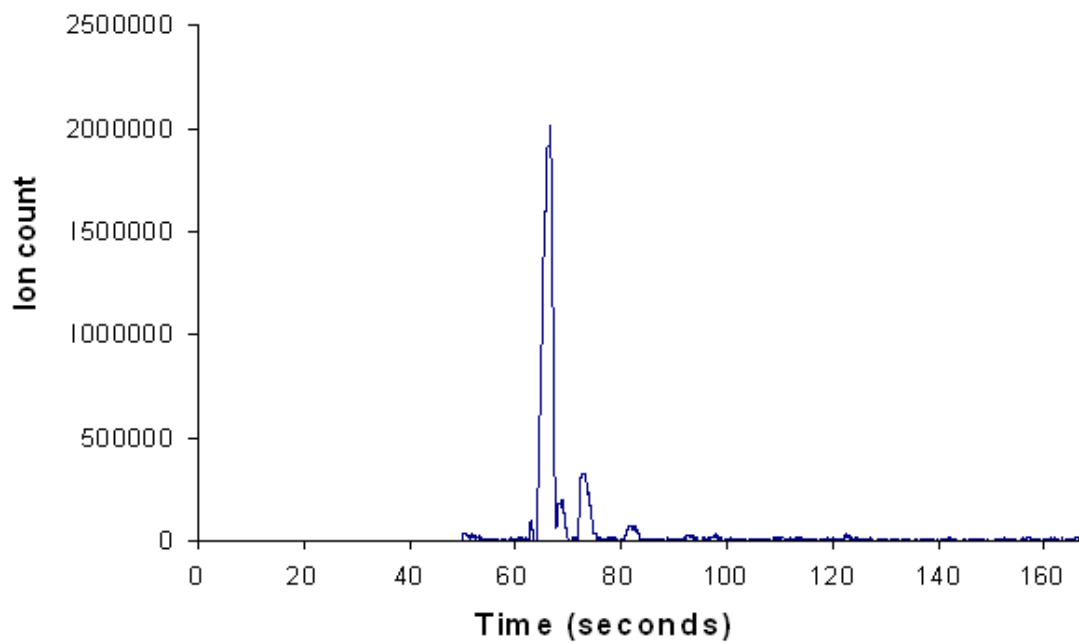


Figure 3.3. Chromatogram for trap blank

3.2. Bag sampling

A 0.05 μL volume of the mixture of four straight chain alkanes (hexane, heptane, octane, and nonane) and two straight chain aldehydes was injected into 1L Tedler bags that were washed and filled with nitrogen. The bags were attached to the sampling system of the sorbent trap, and sampling was accomplished using at different time intervals. The same procedure was also used for 5L and 100L bag sampling. The layout of the sampling system is shown in Figure 3.4.

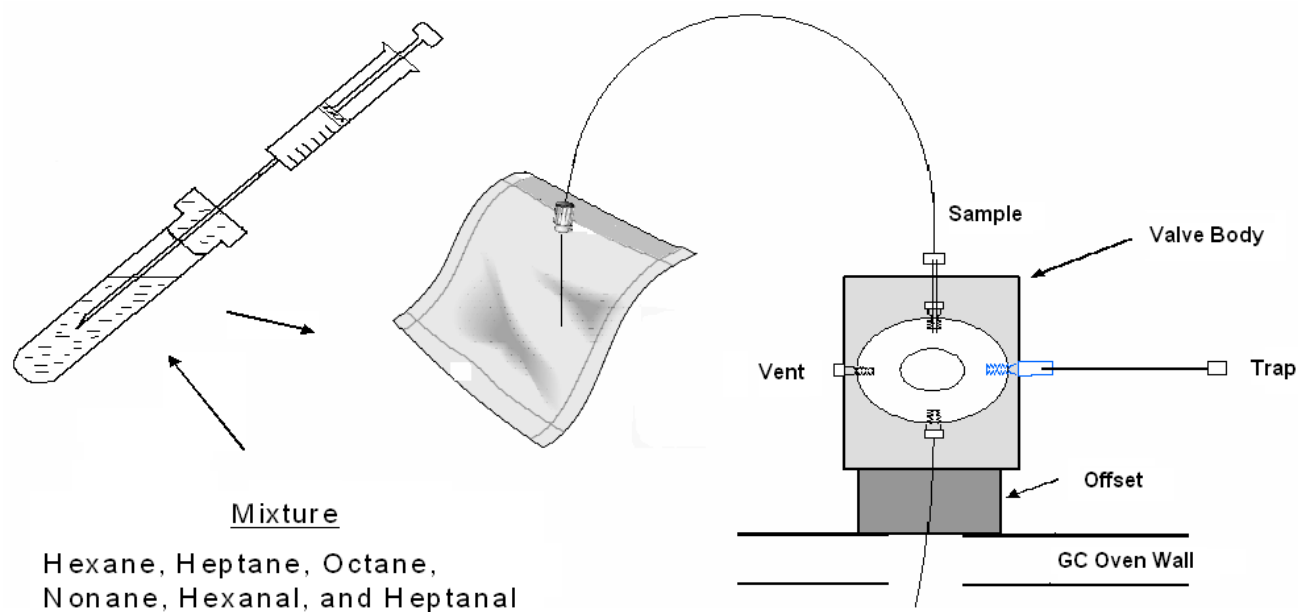


Figure 3.4. Bag sampling of the mixture

3.2.1. Data for 1L bag sampling

Chromatograms for the mixture at 15 sec, 20 sec, 25 sec, 30 sec, 40 sec, and 60 sec sampling times in 1L bag are shown in Figure 3.5 through 3.10, respectively. Straight chain alkanes were the first compounds to appear, followed by straight chain aldehydes. The alkanes show gaussian peaks and were separated with good peak resolution at 15 and 25 second sampling times. As the sampling time increased, the aldehydes begin to appear, though there is partial collection with alkanes. Additionally the peak shapes of the alkanes become distorted. It appears that the low molecular weight compounds did not retain well on the trap as the sampling time increased. In the case of 1L bag sampling, the optimum sampling time for alkanes was 25 seconds where all the compounds were retained well on the trap. Aldehydes required longer sampling times, optimizing at 40 seconds for this concentration. The peak near 100 seconds in all of these chromatograms is the sampling peak that was observed in both room and bag blanks.

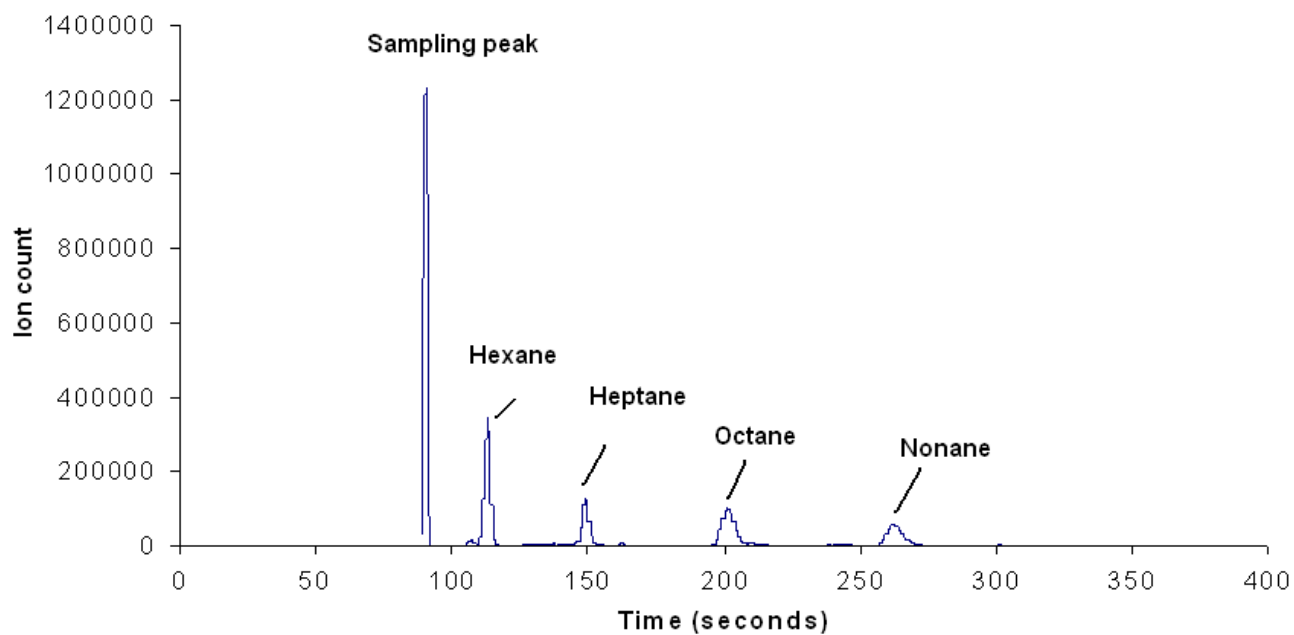


Figure 3.5. Chromatogram for the mixture at 15 sec sampling time.

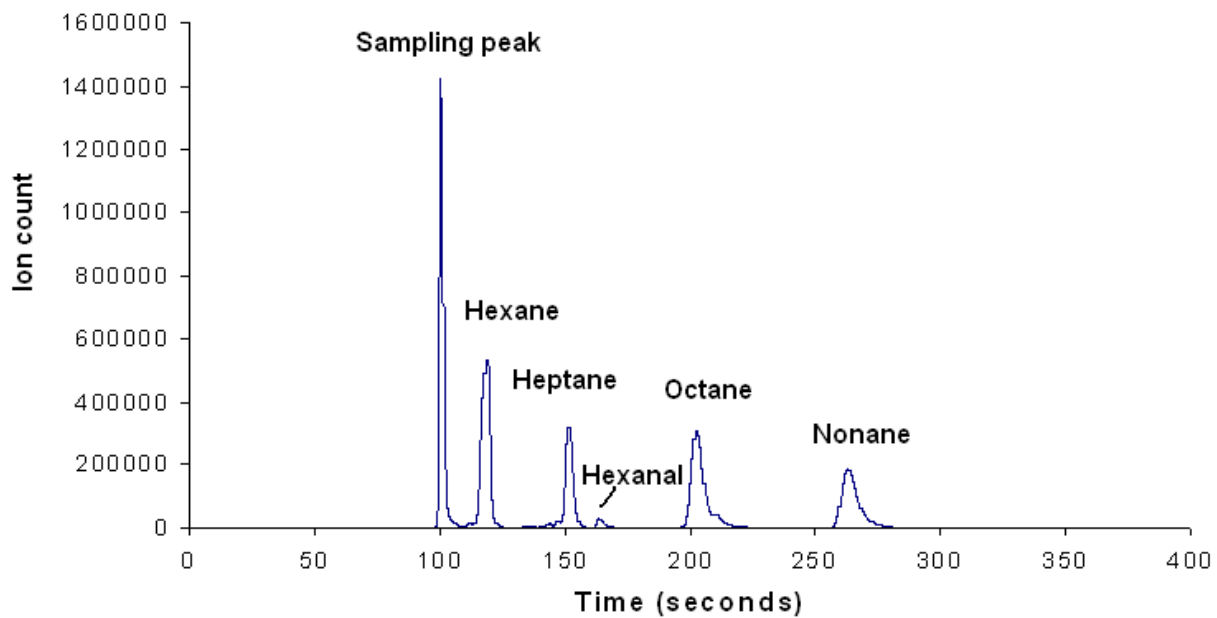


Figure 3.6. Chromatogram for the mixture at 20 sec sampling time.

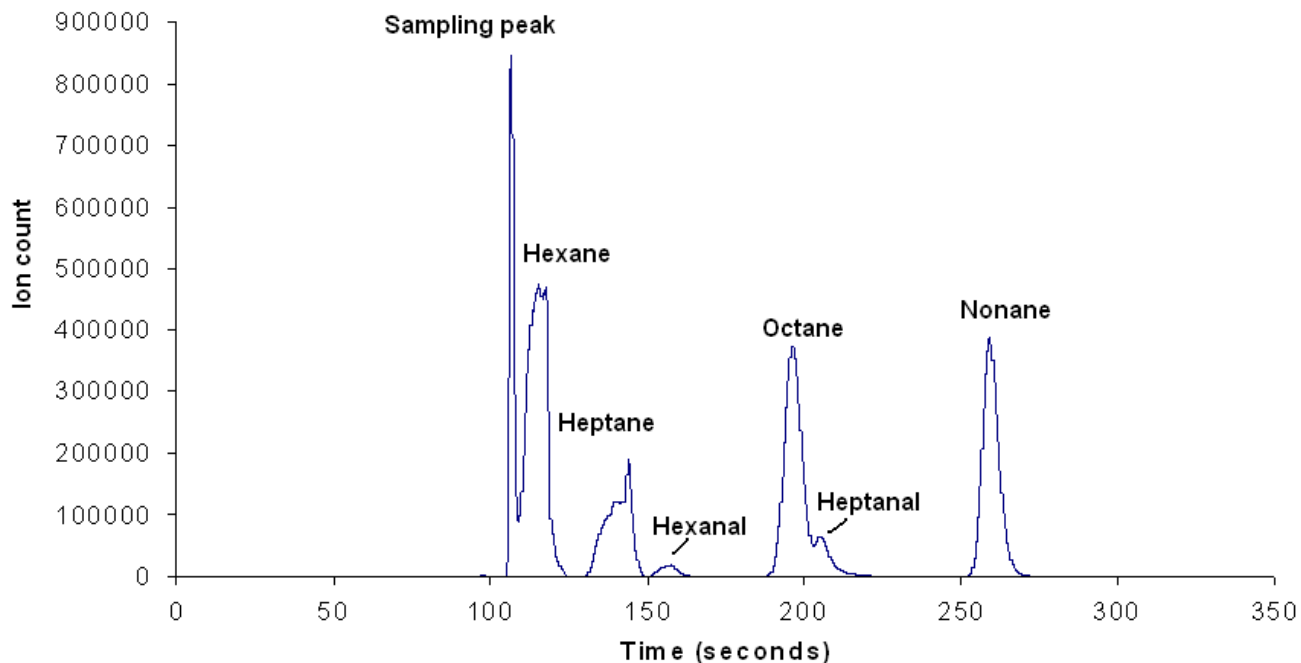


Figure 3.7. Chromatogram for the mixture at 25 sec sampling time.

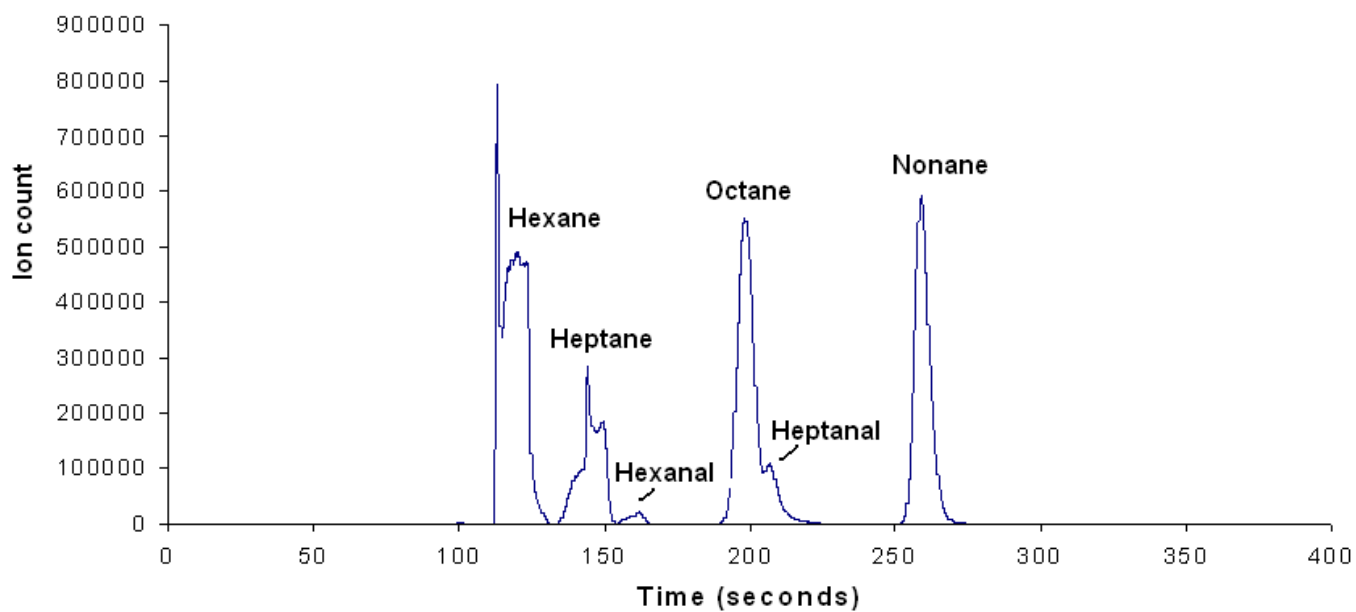


Figure 3.8. Chromatogram for the mixture at 30 sec sampling time.

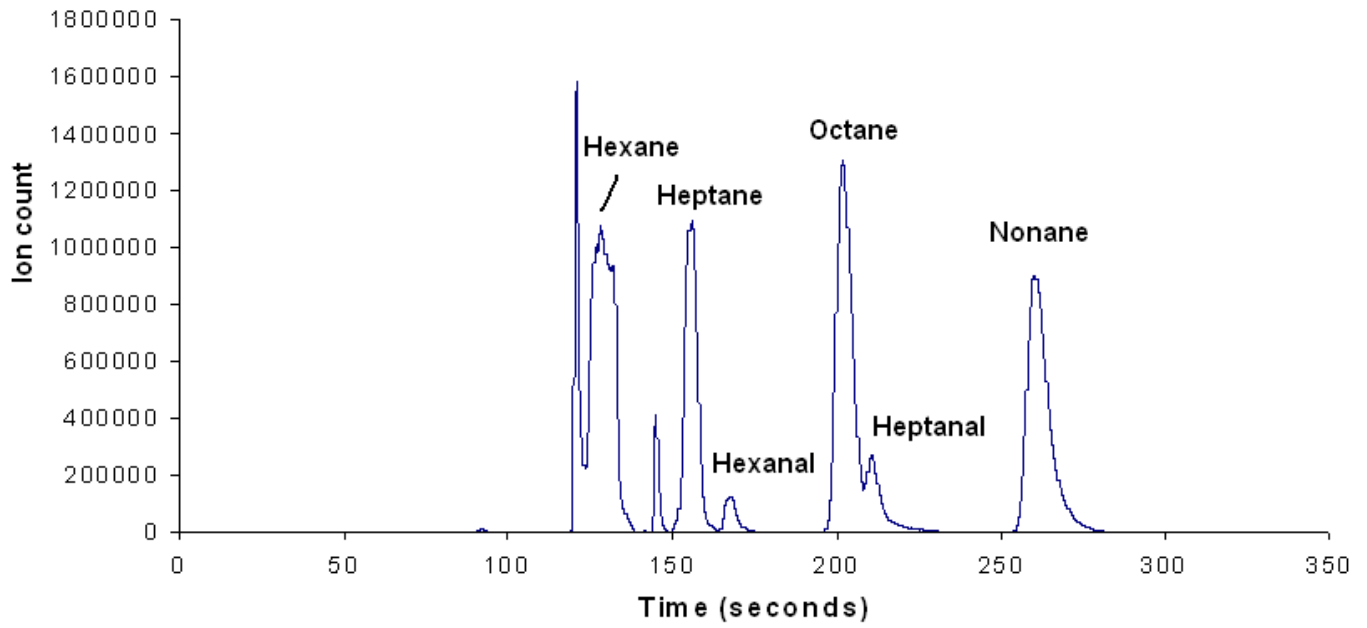


Figure 3.9. Chromatogram for the mixture at 40 sec sampling time.

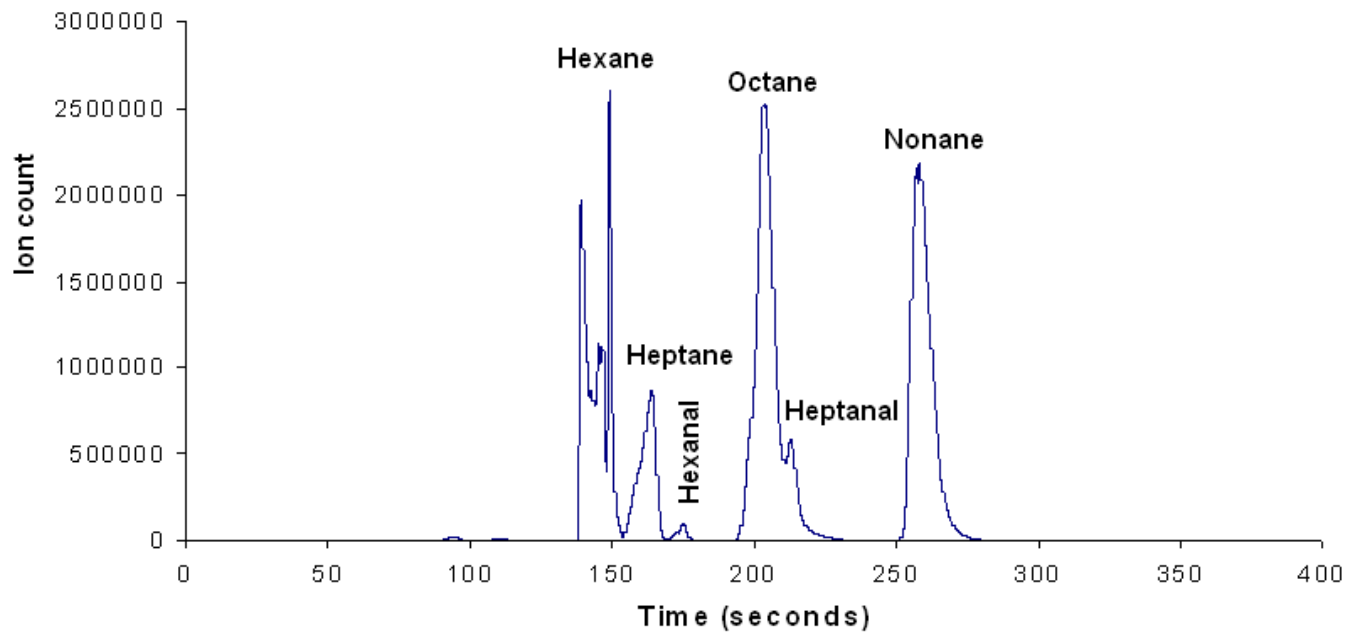


Figure 3.10. Chromatogram for the mixture at 60 sec sampling time.

3.2.2. Data for 5L bag sampling

Chromatograms for the mixture at 15 sec, 20 sec, 30 sec, 40 sec, 50 sec, and 60 sec sampling times in 5L bag are shown in Figures 3.11-3.16, respectively. The lower concentration is reflected in smaller peak areas than those in Figures 3.5 -3.10. The general progression is similar; with a 15- seconds sampling time, all alkanes are present and Gaussian in shape. With a 20- seconds sampling time, the peak for hexane begins to distort, growing worse as the sampling time increases. In contrast, heptane remains Gaussian, distorting at 60- seconds sampling time. The peak for heptanal grew steadily as expected. Peaks for octane and nonane were Gaussian and grew steadily as before.

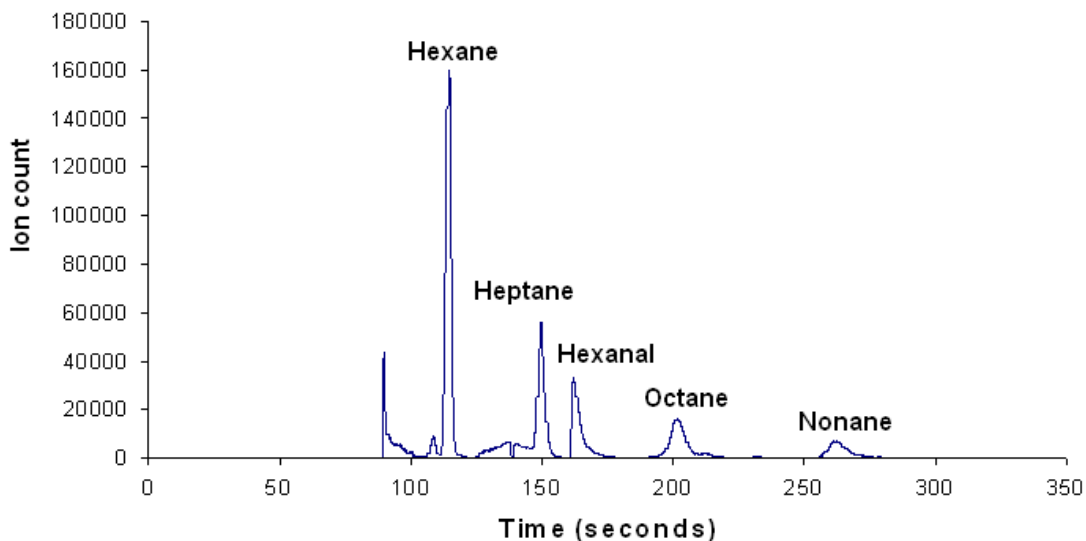


Figure 3.11. Chromatogram for the mixture at 15 sec sampling time.

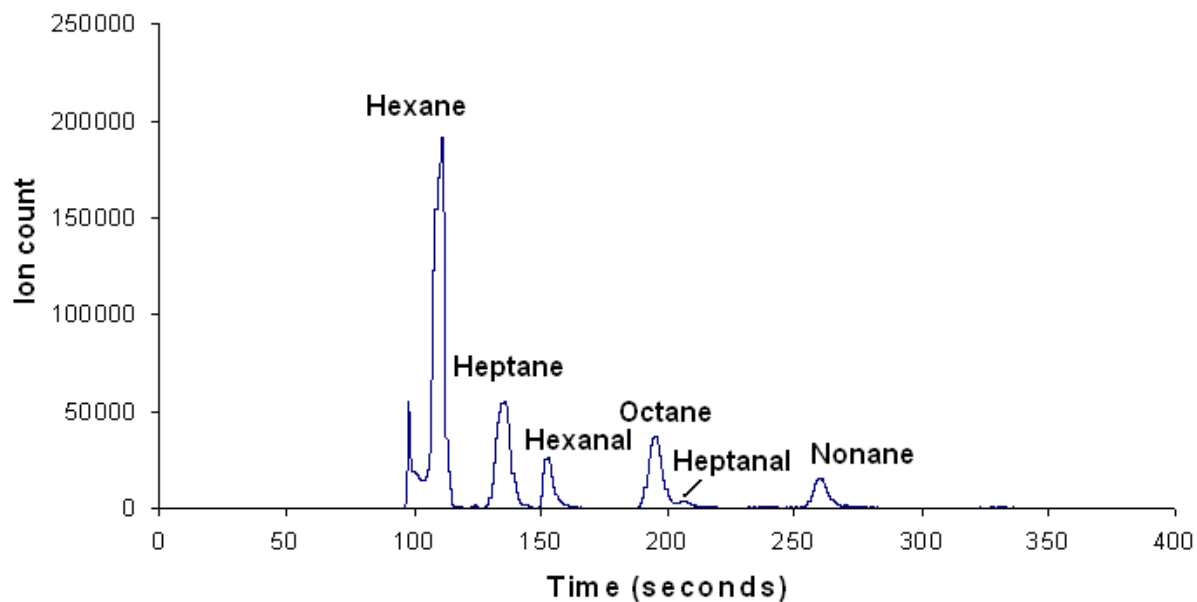


Figure 3.12. Chromatogram for the mixture at 20 sec sampling time.

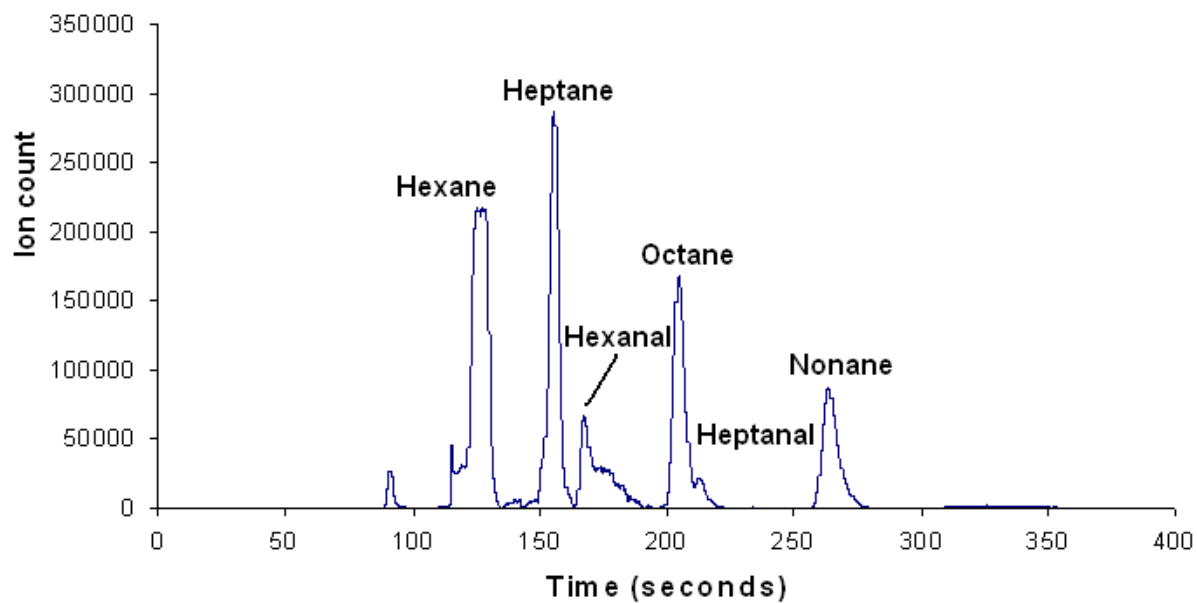


Figure 3.13. Chromatogram for the mixture at 30 sec sampling time.

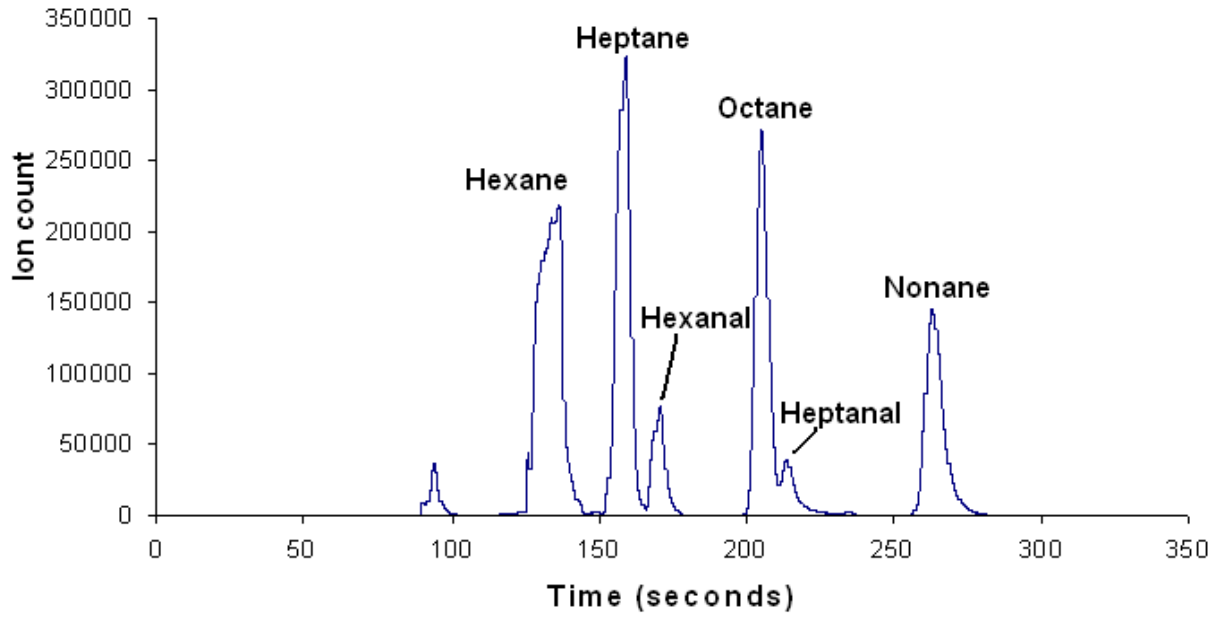


Figure 3.14. Chromatogram for the mixture at 40 sec sampling time.

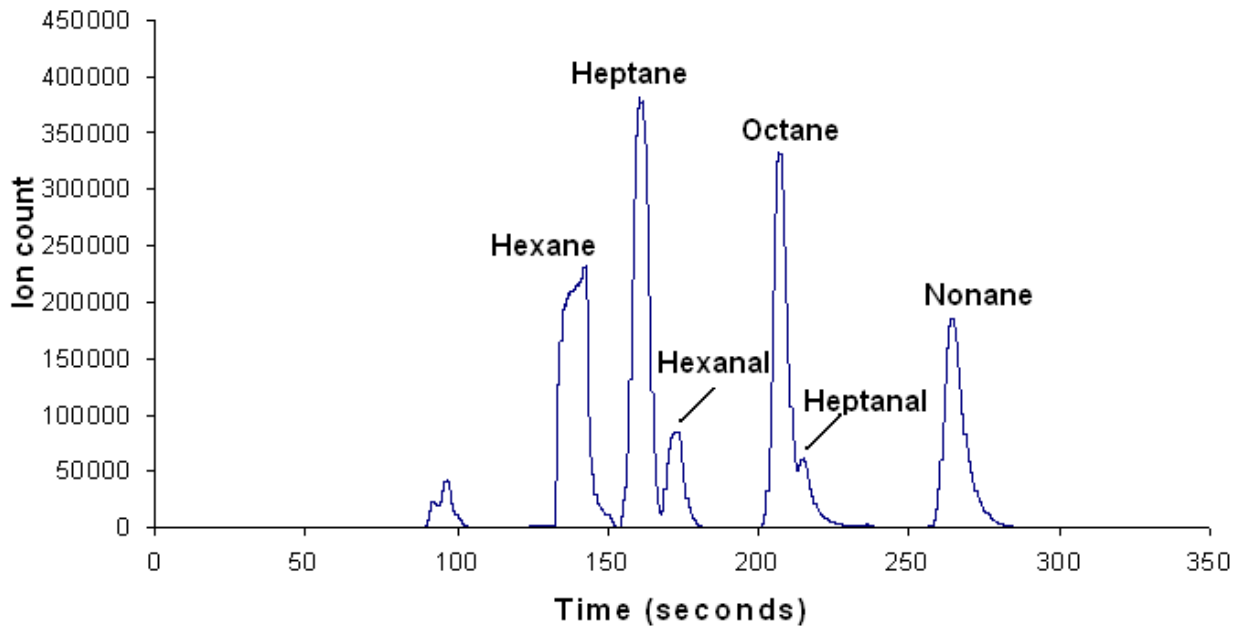


Figure 3.15. Chromatogram for the mixture at 50 sec sampling time.

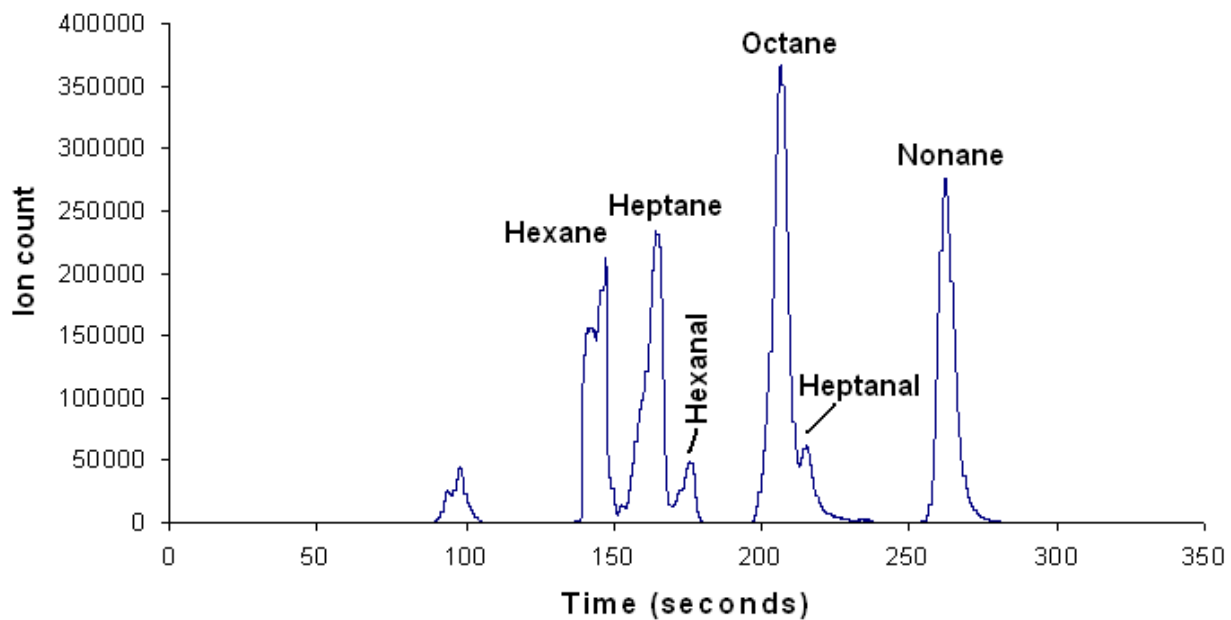


Figure 3.16. Chromatogram for the mixture at 60 sec sampling time.

3.2.3. Data for 100L bag sampling

Chromatograms for the mixture at 20- sec, 30- sec, 40- sec, and 60- sec sampling times in 100L bag are shown in Figures 3.14 - 3.17, respectively. At a 20- seconds sampling time, hexane is Gaussian. With a 30- seconds sampling time and longer, the peaks for hexane are distorted. Heptane begins to distort at 40 seconds, which is earlier than with the 5L bag. Octane and nonane remain Gaussian throughout and grow steadily. Heptanal grows steadily, but does show tailing.

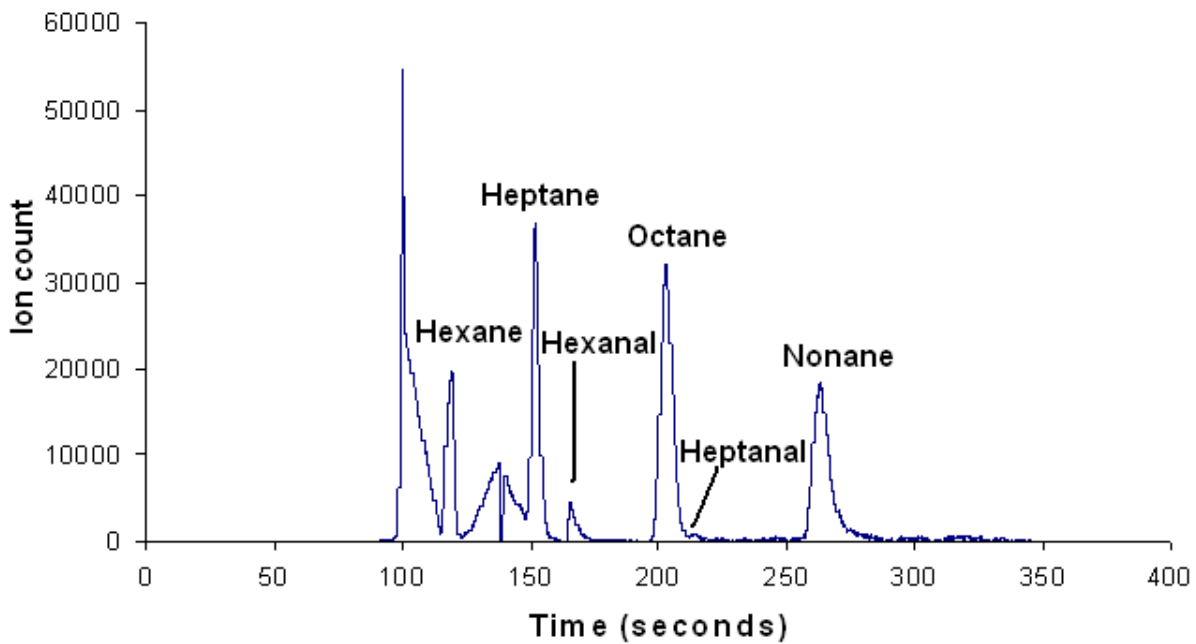


Figure 3.14. Chromatogram for the mixture at 20 sec sampling time.

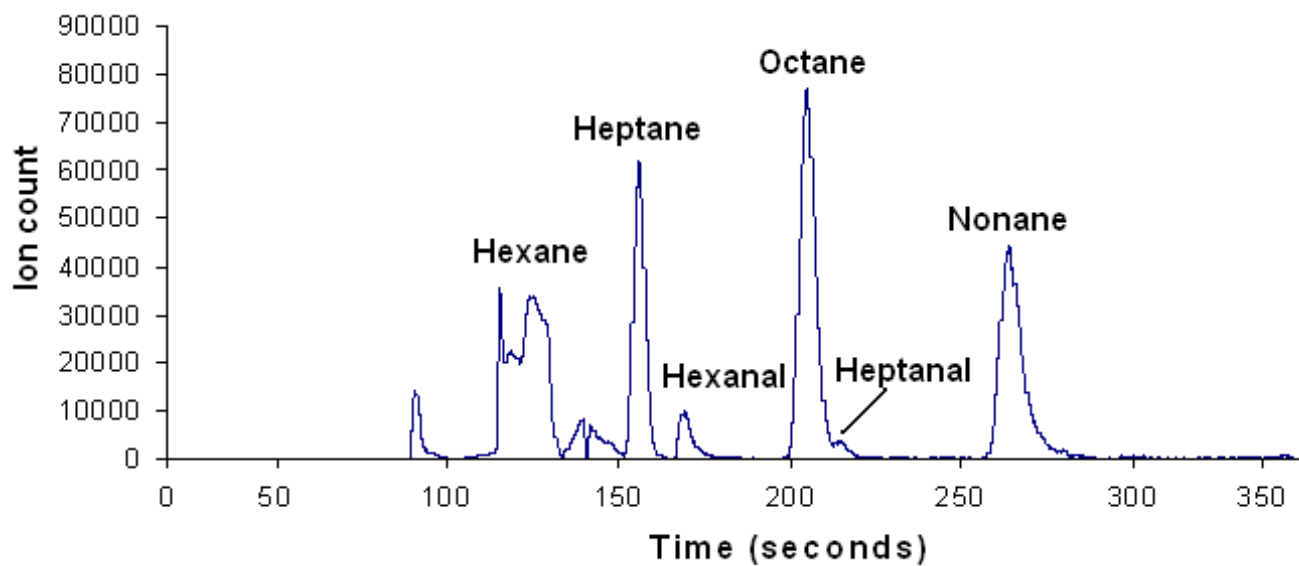


Figure 3.15. Chromatogram for the mixture at 30 sec sampling time

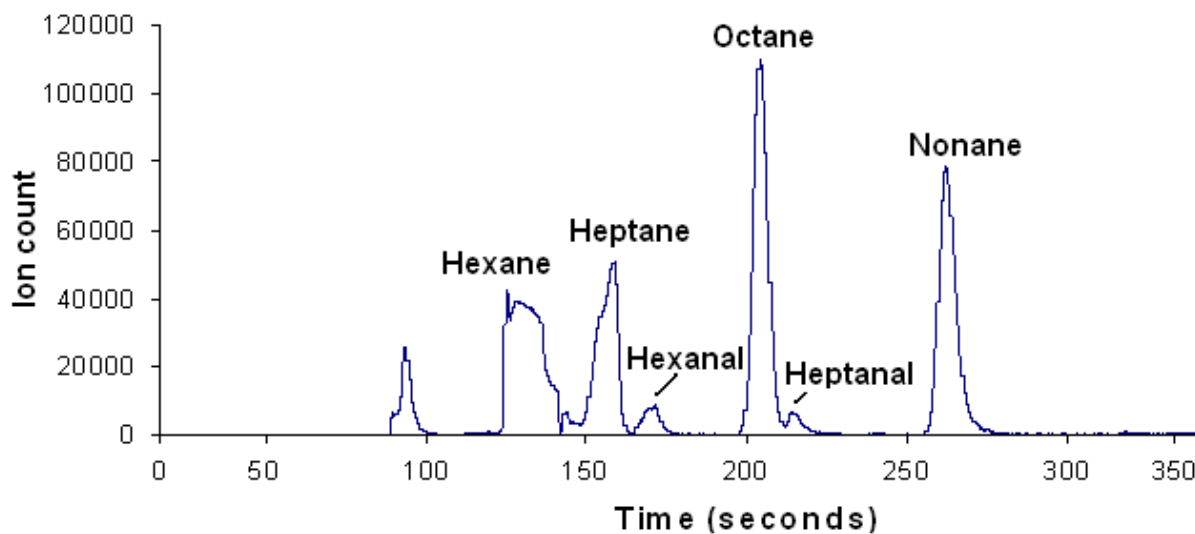


Figure 3.16. Chromatogram for the mixture at 40 sec sampling time.

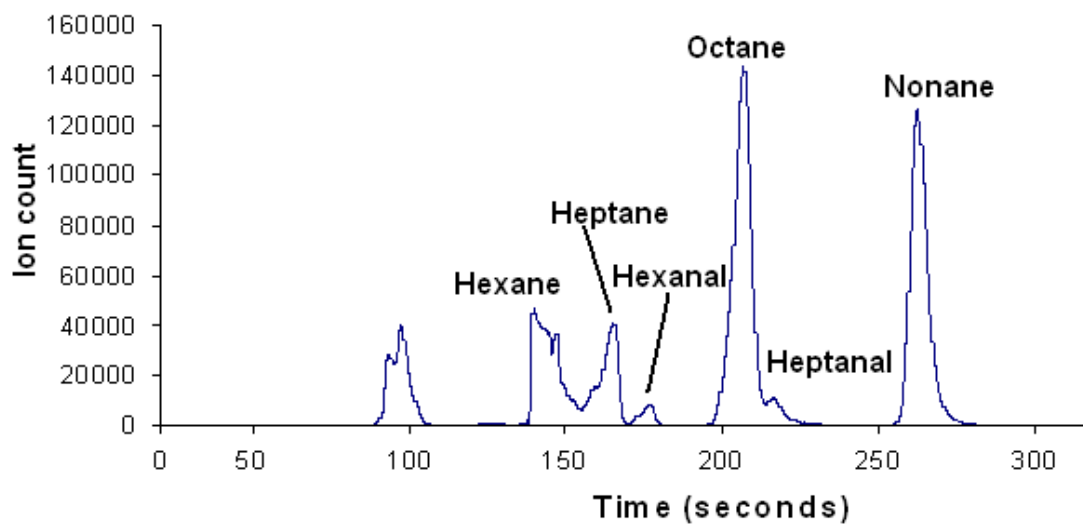


Figure 3.17. Chromatogram for the mixture at 60 sec sampling time.

A very important consideration in trap design was the amount of sample vapor that could be held by the trap and the amount of time that the sample could spend before the sample loss from the trap because of the breakthrough effect. Sample breakthrough volumes are dependent on temperature during sample analysis. Mitra et al. [44] used sub-ambient temperatures during their analysis of VOCs and, using sorbent traps, found that low temperatures would reduce the risk of breakthrough

The mass of analytes collected in the sorbent trap can be changed by changing the sample collection time. As the sampling time increased, the low molecular weight compounds or highly volatile compounds that did not retain well on the trap entered into the GC column. This resulted in saturation of the column as well as irregular peak areas and shapes.

CHAPTER 4

CONCLUSIONS

In recent years GC-MS has become one of the most popular and widely used analytical methods for the determination of volatile aldehydes that are produced due to lipid peroxidation. Various derivatization methods along with GC-MS have proven to be very useful for the identification and quantification of lipid peroxidation products, but the real time analysis of lipid peroxidation products is not possible with these techniques.

Multibed sorbent trap coupled with GC-MS can be a very useful and effective online preconcentration device for the analysis of VOCs that are generated due to lipid peroxidation. Due to the strength of the sorbents used to construct the traps used in these studies, the compound volatility range was limited to about C₉ alkanes and C₇ aldehydes. The optimum sampling time (and therefore the level of pre concentration) is governed by the concentration of sample being drawn to the trap, and the volatility of the compounds, necessitating optimization for each application.

An additional consideration is that currently, traps must be constructed by hand until the builder has experience; reproducibility is not typically acceptable. A more robust method for construction is required.

A major advantage of the preconcentration described in this work is that it is operated online without the need for a conventional GC inlet. This creates the need for additional focusing devices, inlet splitters, and temperature automation. The online sorbent trap should be useful for a variety of applications, including VOCs analysis of lipid peroxidation.

CHAPTER 5

DESIGN OF A METAL CLOSING

5.1 Design of a Metal Closure for the Use of Multibed Sorbent Traps with Gas Chromatography–Time of Flight Mass Spectrometry (GC-TOFMS)

To improve the sensitivity of the sorbent trap that is coupled with GC-MS, there is a great need to design a metal closure that would connect the four port valve system and sorbent trap directly to the GC column. The metal closure placement and the cross section of the metal closure are described in Figures 1 and 2 .

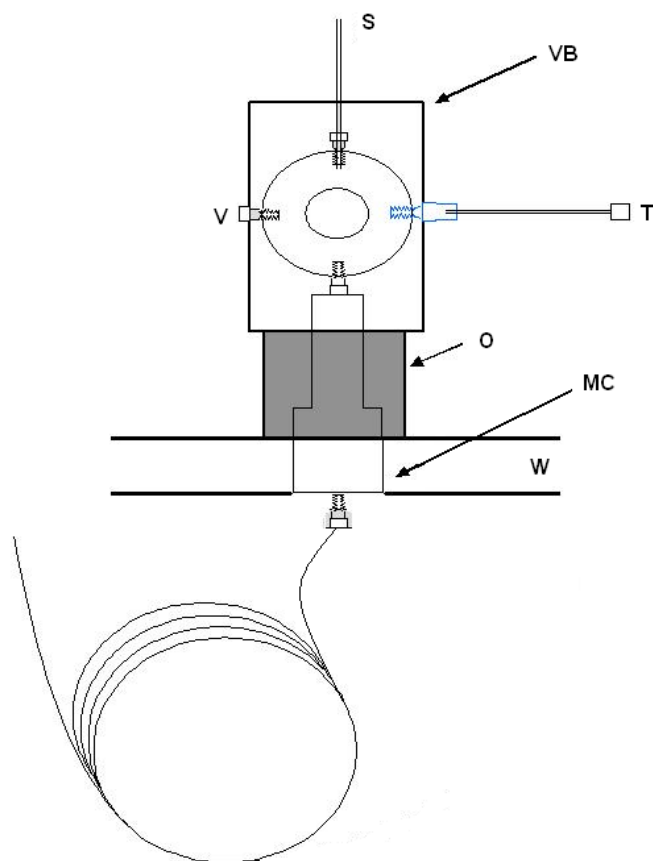


Figure 5.1. Metal closure system with four port valve and sorbent trap.

The instrument set-up consists of sample system (S), valve body (VB), trap (T), vent (V), valve offset (O), and metal closure (MC). The total set-up is connected to the GC column by placing the whole set up on the GC oven wall (W) to connect the trap directly to the four- port valve and the GC column. The main advantage of connecting the valve and sorbent trap directly to the GC column by metal closure is that a low concentration of O₂ enters into the system compared to GC-MS-Sorbent trap set-up without metal closure.

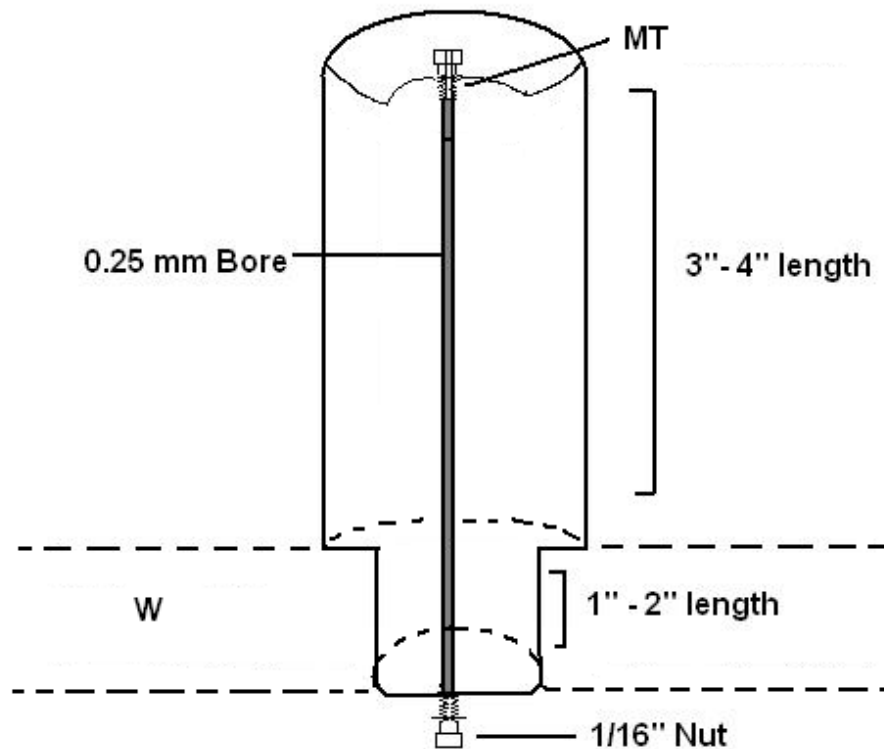


Figure 5.2. Cross sectional view of the metal closure.

The cross-sectional view of the metal closure include 3-4 inches length aluminum cylinder with a 0.25 mm bore. To fit the orifice of the GC wall, the metal cylinder is welded with 1-2 inches length metal tube. The GC end of the metal tube is fitted with 1/16th inch nut to connect with the GC column, and the other end of the cylinder is fitted with male threading nut to connect with the four- port valve system.

The metal closure system should prove very useful to improve the sensitivity of the GC-MS-Sorbent trap system by eliminating dead volumes and cold spots in the system.

References:

- 1) Luvizotto-Santos, R.; Lee, J.; Branco, Z.; Bianchini, A.; Nery, L. *J. Exp. Zoolog A Comp Exp Biol.* **2003**, 295 (2), 200-205.
- 2) DeMartinis, F. D.; Francendese, A. *J Lipid Res.* **1982**, 23(2), 1107-1120.
- 3) Roderick, S. L.; Chan, W.W.; Agate, D. S.; Olsen, L. R.; Vetting, M. W.; Rajashankar, K. R.; Cohen, D. E. *Nat Struct Biol.* **2002**, 9(7), 507-511.
- 4) Bettelheim, F.; Brown, W. H.; March, J.; *Introduction to Organic & Biochemistry.* 4th edition. Harcourt College Publisher, **2001**, 229.
- 5) Hein, M.; Best, L.; Pattison, S.; Arena, S. *Introduction to General, Organic, and Biochemistry.* 6th edition. Brooks/Cole Publishing, **1997**, 793-797.
- 6) Halliwell, B.; Gutteridge, J. M. C. *Free Radicals in Biology and Medicine*, 2nd edition, Clarendon Press, **1989**, 10-15.
- 7) Luo, X. P.; Yazdanpanah, M.; Bhoo, N.; Lehotay, D. C. *Anal. Biochem.* **1995**, 228, 294-298.
- 8) Moore, K.; Roberts L. J. *Free Rad. Res.* **1998**, 28, 659-671.
- 9) Liu, J.; Doniger, S. J.; Ames, B. N. *Anal. Biochem.* **1997**, 245, 161-166.
- 10) Poli, G.; Albino, E.; Dianzani, M.U. *Chem. Phys. Lipids*, **1987**, 45, 117-142.
- 11) Esterbauer, H.; Schauer, R. J.; Zollener, H. *Free Radical Biol.Med.* **1991**, 11, 81-128.
- 12) Janero, D. R. *Free Radical Biol. Med.* **1990**, 9, 515-540.
- 13) Moore, K.; Roberts, L. J. *Free Rad.* **1998**, 28, 659-671.
- 14) Esterbauer, H.; Zollner, H. *Free Radical Biol. Med.* **1989**, 7, 197-203.
- 15) Frankel, E. N.; Hu, M. L. Tappel, A. L. *Lipids.* **1991**, 26, 479-484.

- 16) Carolyn, F.; Goodridge, C. Randolph, M.; Brandry, R. M.; Pestka, J.; Smith, M. J. *Agric. Food Chem.* **2003**, *51*, 4185-4190.
- 17) Denni, K. J.; Shibamoto, T. *Free Rad. Biol. Med.* **1989**, *7*, 187.
- 18) Bird, R. P.; Hung, S.; Hadley, M.; Draper, H. *Anal. Biochem* **1999**, *128*, 240-244.
- 19) Luo, X. P.; Yazdanpanth, M.; Bhooi. N.; Lehotay, D.C. *Anal. Biochem* **1995**, *228*, 294-298.
- 20) Des Rosiers. C.; Rivest, M. J.; Bioly, M. J.; Jette, M.; Carrobe-Cohen. A. *FASEB J.* **1991**, *6*, A1341.
- 21) Des Rosiers. C.; Rivest, M. J.; Bioly, M. J.; Jette, M.; Carrobe-Cohen. A.; Kumar. A. *Anal. Biochem* **1993**, *208*, 161-170.
- 22) Giddings, J. C. *Unified Separation Science*. Wiley, Newyork, **1991**, 237.
- 23) McNair, M.; Miller, J. M. *Basic Chromatography*; John Wiley & Sons Inc.: New York. **1998**. 255-259.
- 24) Golay, M. J. E.; *Gas Chromatography*, **1997**, Lansing symposium, Academic press, New York.
- 25) Sanchez, J. M.; Sacks, R.D. *Anal. Chem.* **2003**, *75*, 2231-2236.
- 26) Trehy, M. L.; Gledhill, W.E.; Mieure J. P. *Environmental Toxicology and Chemistry*, **1996**, *15(3)*, 233-240.
- 27) Amunugama, M.; Clifford, C.D.; Gutman, P. M.; Soltani, M.; Karunaratne, S.; Venkatachalam, K.; Pernecky, S. L.; Holmes, H. L. S. *Chromatographia* **2004**, *60(7-8)*, 441-447.
- 28) Snow, H. N.; Slack, G. C.; *Trends in Analytical Chemistry*, **2002**, *21(9-10)*, 608-617.
- 29) Venema, A.; *J. High. Resolut. Chromatogr.* **1990**, *13*, 537.

- 30) Bianchi, A.; Varney, M. S.; Phillips, J.; *J.Chromatogr.* **1999**, *467*, 111.
- 31) Brymer, D. A.; Ogle, L. D.; Jones, C. J.; Lewis, D. L. *Environ.Sci. Technol.* **1996**, *30*, 188-195.
- 32) Stanshenko, E. E.; Puertas, A. M.; Martinez, J. R. *J. Bioanal Chem.* **2002**, *373(1-2)*, 70-74.
- 33) Carolyn, F.; Goodridge, C.; Randolph, M.; Brandry, R. M.; Pestka, J.; Smith, M.; *J. Agric. Food Chem.* **2003**, *51*, 4185-4190.
- 34) Moore, K.; Holt, S. *Biological Chem.* **1998**, *273*, 31731-31737
- 35) Yeo, H. C.; Liu, J.; Helbock, H. J.; Ames, B. N. *Methods Enzymol* **1999**, *300*, 70-78
- 36) Ozawa, A. *J.Chromatogr.* **1993**, *644*, 375-382.
- 37) Burlingame, A. L.; Boyd, R. K.; Gaskell, S. J. *Anal.Chem.* **1998**, *70*, R647-716.
- 38) Wollink, H.; Becker, H.; Gotz, H.; Kraft, A.; Jung, H.; Chen, C.C; Vanysacker, P.G.; Jansen, H. G. *Intl.J.Mass.Spectrom.Ion.Proc.* **1994**, *130*, L7-L11.
- 39) Holland, J. F.; Emke, C. G.; Allison, J.; Stults, J. T.; Pinkston, J. D.; Newcome, B.; Watson, J. T. *Anal. Chem.* **1983**, *55*, 997A.
- 40) Wollink, H. *Mass Spectrom. Rev.* **1993**, *12*, 89-114.
- 41) Erickson, E. D.; Enke, C. G.; Holland, J. F.; Watson, J. T. *Anal. Chem.* **1990**, *62*, 1079-1084.
- 42) Watson, J. T.; Schultz, G. A.; Tecklenburg, R. E.; Allison, J. *J. Chromatogr.* **1990**, *518*, 283-295.
- 43) Schultz, G. A.; Chamberlin, B. A.; Sweeley, C. C.; Watson, J. T.; Allison, J. *J. Chromatogr.* **1992**, *590*, 329-339.
- 44) Mitra. S.; Xu.Y.; Chen. W.; Lai. A. *J. Chromatogr. A*, **1996**, *727*, 111-118

- 45) Mitra, S.; Yun, C. *J. Chromatogr.* **1993**, *648*, 415
- 46) Mitra, S.; Lai, A. *J. Chromatogr. Sci.* **1995**, *33*, 285
- 47) Sanchez, J. M.; Sacks, R.D. *Anal. Chem.* **2003**, *75*, 2231-2236
- 48) Lu, C.; Zellers, E. *Anal. Chem.* **2001**, *73*, 3449-3457.
- 49) Lu, C.; Zellers, E. *Analyst* **2002**, *127*, 1061-1068.
- 50) Sanchez, J. M.; Sacks, R.D. *Anal. Chem.* **2003**, *75*, 978-985.